Control of Gliotactin localization and levels by tyrosine phosphorylation and endocytosis is necessary for survival of polarized epithelia

Mojgan Padash-Barmchi, Kristen Browne, Kendra Sturgeon, Barbara Jusiak and Vanessa J. Auld*

Department of Zoology, Cell and Developmental Biology, University of British Columbia, Vancouver, Canada BC V6T 1Z3

*Author for correspondence (auld@zoology.ubc.ca)

Accepted 9 August 2010
Journal of Cell Science 123, 4052-4062

doi:10.1242/jcs.066605

Summary

The tricellular junction (TCJ) forms at the convergence of bicellular junctions from three adjacent cells in polarized epithelia and is necessary for maintaining the transepithelial barrier. In the fruitfly *Drosophila*, the TCJ is generated at the meeting point of bicellular septate junctions. Gliotactin was the first identified component of the TCJ and is necessary for TCJ and septate junction development. Gliotactin is a member of the neuroligin family and associates with the PDZ protein discs large. Beyond this interaction, little is known about the mechanisms underlying Gliotactin localization and function at the TCJ. In this study, we show that Gliotactin is phosphorylated at conserved tyrosine residues, a process necessary for endocytosis and targeting to late endosomes and lysosomes for degradation. Regulation of Gliotactin levels through phosphorylation and endocytosis is necessary as overexpression results in displacement of Gliotactin away from the TCJ throughout the septate junction domain. Excessive Gliotactin in polarized epithelia leads to delamination, paired with subsequent migration, and apoptosis. The apoptosis and the resulting compensatory proliferation resulting from high levels of Gliotactin are mediated by the *Drosophila* JNK pathway. Therefore, Gliotactin levels within the cell membrane are regulated to ensure correct protein localization and cell survival.

Key words: Septate junction, Tricellular junction, *Drosophila*, Tyrosine phosphorylation, Endocytosis, JNK

Introduction

Establishment and maintenance of cellular permeability barrier is important for preservation of the integrity of epithelia. In epithelial cells of invertebrates, permeability barriers are formed by pleated septate junctions (SJs), which are functionally analogous to tight junctions in vertebrates (Noirot-Timothee et al., 1982; Tsukita et al., 2001). In *Drosophila*, SJs form ladder-like junctions between cells in a region just basal to the adherens junctions. The multi-stranded nature of SJs effectively prevents the paracellular flow of molecules. Several SJ proteins have been identified that are important for development of these junctional domains. Mutations in the genes encoding any of these components, including *Neurexin-IV* (Baumgartner et al., 1996), *coracle* (Fehon et al., 1994), *Neuroglian* and the *Na+/K+ ATPase* (Genova and Fehon, 2003; Paul et al., 2003), block the formation of SJ strands.

Analysis of epithelial cells with electron microscopy has shown that the continuity of SJ strands is interrupted at the convergence point of three cells (Fristrom, 1982; Noirot-Timothee et al., 1982). This junction, known as the tricellular junction (TCJ), is also vital to create an intact permeability barrier to ensure that solutes fail to flow in the channel formed between the three cell corners. The permeability barrier at the TCJ is created by a series of diaphragms that might act as anchors for SJ strands (Fristrom, 1982; Noirot-Timothee et al., 1982). So far in *Drosophila*, only one protein, Gliotactin (Gli), is found specifically localized at the TCJ. In Gliotactin mutants, SJ strands form but fail to compact, and this, combined with a disrupted TCJ, results in a defective transepithelial barrier and embryonic lethality (Schulte et al., 2003). Gliotactin is a cholinesterase-like molecule with an extracellular serine esterase domain that lacks enzymatic activity (Gilbert et al., 2001; Gilbert and Auld, 2005). In the intracellular domain, Gliotactin contains a PDZ binding motif that has previously been shown to form a protein complex with discs large through a currently unknown linker protein (Schulte et al., 2006).

In addition to the PDZ binding motif, the cytoplasmic domain of Gliotactin also contains two predicted and highly conserved tyrosine phosphorylation sites at amino acids 766 and 790. Phosphorylation by tyrosine kinases plays an important role in internalization and endocytosis of many membrane proteins, including receptor tyrosine kinases (RTKs), insulin receptors and cell adhesion proteins such as E-cadherin (Ahmadian et al., 2004; Behrens et al., 1993; Ivanov et al., 2005; Takeda et al., 1995; Tanos and Pendergast, 2006). As such, endocytosis plays a crucial role in the downregulation of signaling and changes in membrane protein composition. For instance, tyrosine phosphorylation of cadherins is needed for endocytosis and destruction of adherens junctions during the epithelial–mesenchymal transition (Behrens et al., 1993). However, there was no prior evidence that tyrosine phosphorylation and endocytosis are important for SJ formation and maintenance.

Here, we show that phosphorylation of the conserved tyrosines in the intracellular domain of Gliotactin results in endocytosis and targeting to late endosomes and lysosomes for degradation. The expression level of Gliotactin and unique localization to the TCJ are regulated through phosphorylation and subsequent endocytosis. Tight control is necessary, as the displacement of Gliotactin away from the TCJ throughout the SJ domain leads to delamination, migration and apoptosis of columnar epithelial cells in imaginal discs. We show that the JNK pathway mediates the cell death and proliferation resulting from high levels of Gliotactin. Therefore,

Journal of Cell Science

Gliotactin levels within the cell membrane are regulated to ensure correct protein localization and cell survival.

Results

Tyrosine phosphorylation sites in Gliotactin are necessary for endocytosis

The intracellular domain of Gliotactin (Gli) contains a PDZ recognition sequence, shown to associate with Discs large (Dlg) in a complex at the TCJ, and two predicted tyrosine phosphorylation sites at amino acids 766 and 790 (Schulte et al., 2006). These tyrosine phosphorylation sites are strongly conserved, in particular Tyr766, which is found in all Gliotactin homologs (supplementary material Fig. S1B). To investigate the role of the tyrosine residues in Gliotactin, we used site-directed mutagenesis to alter these residues and generated transgenic lines that carry either Gliotactin with the two tyrosines mutated to phenylalanine or Gliotactin with the two tyrosines replaced by aspartic acid (supplementary material Fig. S1A). The former is a mutant version of Gliotactin that should produce a constitutive state of dephosphorylation (GliFF), and the latter is a form that should mimic phosphorylation and be in a constitutive state of phosphorylation (GliDD) (Cantarelli et al., 2007; Cuevas et al., 2001; Huh et al., 2004; Meyer et al., 2003). As a control, we generated a wild-type Gliotactin construct (GliWT), and all three constructs were placed under the control of the GAL4 upstream activating sequence (UAS) sequence (Brand and Perrimon, 1993).

In order to see whether any of these transgenes are able to rescue the embryonic lethality of *Gli* mutants, we expressed each construct in a homozygous *Gli* null mutant background, $Gli^{AE2\Delta45}$, using the daughterless GAL4 line (da–GAL4), which drives expression in all tissues. All transgenes including the wild-type form of Gli with intact tyrosine sites (GliWT) were able to fully rescue the embryonic lethality of $Gli^{AE2\Delta45}$ mutants. Two independent lines were used for each to control for differences arising from the position of the transgene insertion. Rescued embryos developed into larval stages, but the majority of larvae became paralysed and died. Some progeny survived to adulthood, but adult flies exhibited malformed leg phenotypes and failed to inflate their wings (supplementary material Fig. S2).

To visualize the localization of Gliotactin in the rescued larvae, we used wing imaginal discs as they provide a powerful system to study the structure of both septate junctions and TCJs. In wild-type discs, Gliotactin is clearly localized at the TCJ of the columnar epithelial cells (Fig. 1A,B), as well as being found in intracellular vesicles (Fig. 1B insert, arrow). For each transgene, Gliotactin was localized to the TCJ in the rescued larvae but also spread throughout the entire SJ owing to the elevated expression levels generated with the daughterless GAL4 driver (Fig. 1D–F). Interestingly, GliWT and GliDD were also found in large intracellular vesicles in comparison with those of GliFF, which was only present at the cell membrane (Fig. 1, arrows in D and E). These observations suggested that the tyrosine phosphorylation could be necessary for Gliotactin endocytosis but did not rule out the possibility that the presence of Gli-containing vesicles resulted from slow intracellular trafficking. We therefore immunolabeled rescued wing discs for Golgi markers and found no association of Gliotactin vesicles with the Golgi apparatus (supplementary material Fig. S3A–C). These results suggested that Gliotactin-containing vesicles are not blocked during trafficking to the plasma membrane. Rather, this suggested that the presence of Gliotactin-positive intracellular vesicles is due to endocytosis

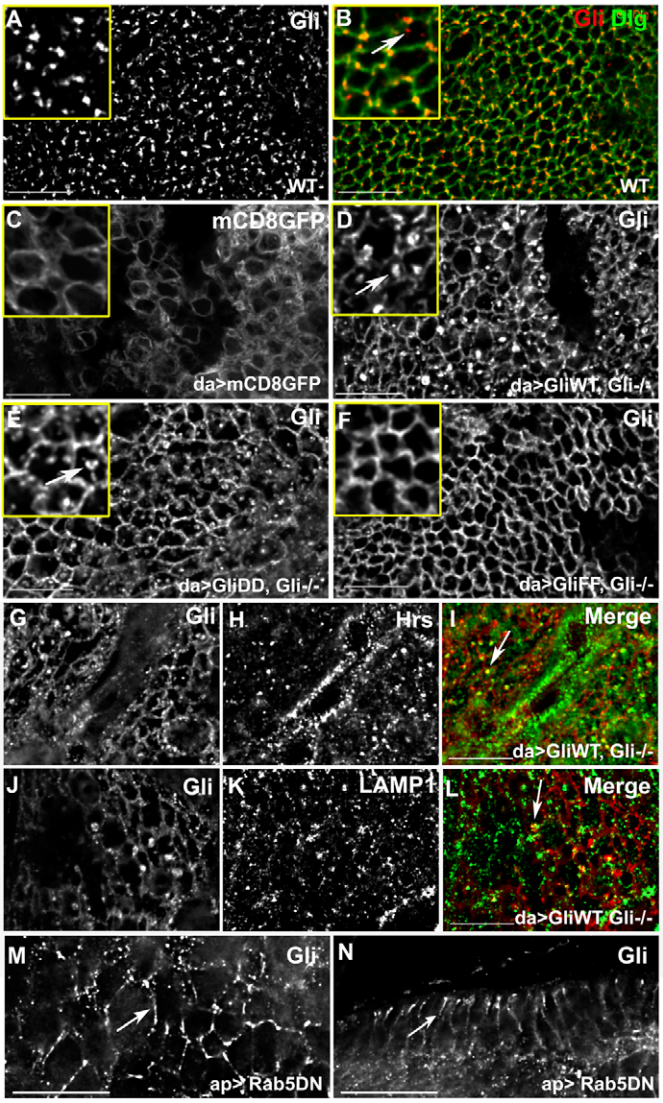

Fig. 1. Gliotactin is endocytosed and targeted to late endosomes and lysosomes. (A–C,M–N) Wild-type wing imaginal discs. (D–L) Rescued wing discs expressing Gliotactin transgenes under the control of daughterless–GAL4 (da–GAL4) in a Gliotactin-null ($Gli^{\Delta45}$) background. (**A**,**B**) Wild-type wing disc, immunolabeled for Gliotactin (red) and Dlg (green). Gliotactin is localized to the TCJ. Inserts in (A) and (B) were digitally scaled by 100%. (**C**) Control wing discs with da–GAL4 driving the expression of the membrane protein mCD8GFP. mCD8–GFP localizes correctly to the plasma membrane, and no intracellular vesicles are detected. (**D–F**) Rescued wing discs expressing GliWT, GliDD and GliFF under the control of da–GAL4 in a Gliotactin-null ($Gli^{\Delta45}$) background. Owing to the strong expression of the da–GAL4 line, Gliotactin spreads through the SJ. GliWT and GliDD exhibit a greater amount of Gliotactin in intracellular vesicles (arrows in D and E) compared with GliFF. Inserts in C–F were digitally scaled by 100%. (**G–I**) A rescued wing disc expressing GliWT (red) under the control of da–GAL4 in a Gliotactin-null ($Gli^{\Delta45}$) background for the endosome marker Hrs (green). Many of the intracellular Gliotactin vesicles were Hrs positive (arrow in I). (**J–L**) A rescued wing disc expressing GliWT (red) under the control of da–GAL4 in a Gliotactin-null ($Gli^{\Delta45}$) background for the lysosomal marker LAMP1 (green). Association of LAMP1 with the large Gliotactin vesicles was observed (arrow in L). (**M**,**N**) Expression of a dominant-negative form of Rab5 (Rab5DN) with apterous–GAL4 in a wild-type wing disc. Endogenous Gliotactin is mislocalized away from the TCJ and found in punctuate structures throughout the SJ domain (arrows). Each panel represents a single *Z* slice. Scale bars: 15 µm.

and that the tyrosine residues of Gliotactin are necessary for this process.

Gliotactin is phosphorylated at tyrosine residues in vivo and in vitro

Our observations prompted us to investigate whether Gliotactin is endogenously phosphorylated at these tyrosine residues. We were unable to detect overlap between phosphotyrosine (phosphoTyr) and Gliotactin in immunolabeled wild-type discs. Therefore, we performed immunoprecipitations on embryos expressing UAS-GliWT under the control of the daughterless–GAL4 driver. Western analysis was carried out using immunofluorescent labeling for simultaneous detection of phosphoTyr residues and Gliotactin (Fig. 2A). A corresponding phosphoTyr band was detected in UAS-GliWT-expressing lines, indicating that Gliotactin is phosphorylated in vivo, possibly at both tyrosines.

To test whether Gliotactin can be phosphorylated in vitro by a tyrosine kinase, we performed Src kinase assays using the human Src–GST fusion paired with purified intracellular domains of Gliotactin (Fig. 2C). Both the wild-type (GliCtermWT) and GliFF (GliCtermFF) intracellular domains were expressed as His-tagged proteins and purified. Tyrosine phosphorylation was detected only for GliCtermWT in the presence of Src. Our negative control in which no Src–GST was present did not show any phosphorylation, and nor did the GliCtermFF protein (Fig. 2C). These results suggest that Src can phosphorylate Gliotactin in vitro at one or both tyrosines.

Gliotactin vesicles are targeted to late endosomes and lysosomes for degradation

To determine whether Gliotactin is targeted for degradation after endocytosis, we immunolabeled wing discs from rescued third-instar larvae with a range of endosomal markers. Endocytosed proteins targeted for degradation traffic to late endosomes, where they are sorted into multivesicular bodies. Multivesicular bodies then fuse with lysosomes, delivering the contents for degradation (Raiborg and Stenmark, 2009). Hrs (Hepatocyte growth factor-regulated tyrosine kinase substrate) plays an important role in this process and is necessary for the maturation of endosomes into multivesicular bodies en route to lysosomes (Jekely and Rorth, 2003; Lloyd et al., 2002). Our immunofluorescence data show colabeling of Hrs with Gliotactin-containing vesicles in the rescued wing discs and some colabeling with the lysosomal marker LAMP1 (Fig. 1G–L, arrows).

In order to confirm the degradation of Gliotactin in our rescue experiments, we performed western blotting on extracts of rescued larvae from all three transgenic lines (Fig. 2B). GliWT and GliDD showed a considerable amount of degradation in comparison with GliFF, which had no degradation (Fig. 2B, arrows). We observed similar degradation products in our control lane, which contained endogenous wild-type Gliotactin. These observations suggest that the phosphoTyr residues in Gliotactin are necessary for endocytosis and might regulate the localization of Gliotactin to the TCJ. In order to investigate this possibility further, we expressed a dominant negative form of Rab5, which has been shown to block endocytosis in a number of *Drosophila* tissues (Marois et al., 2006; Wucherpfennig et al., 2003). In $Rab5^{DN}$-expressing cells, endogenous Gliotactin localization was not restricted to the TCJ and was found throughout the cell membrane as punctate immunolabeling (Fig. 1M,N). These observations suggest that the tyrosine phosphorylation might regulate the amount of Gliotactin present in the membrane and ensure that localization is restricted to the tricellular corners.

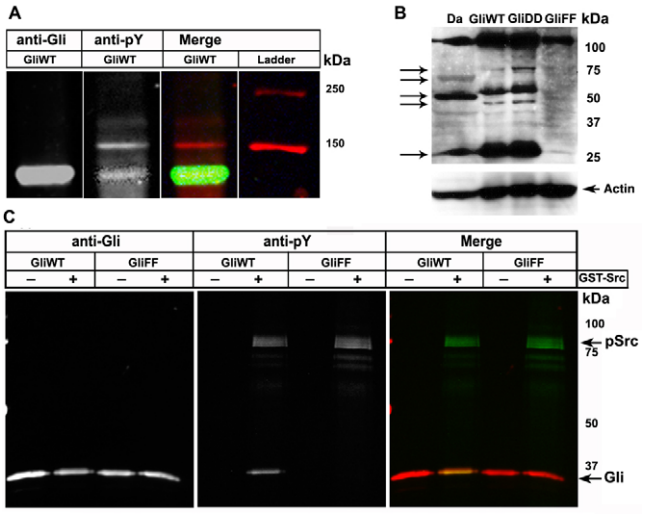

Fig. 2. Gliotactin is phosphorylated at the conserved tyrosine residues. (**A**) Western blot of immunoprecipitations from embryo extracts expressing GliWT under the control of daughterless–GAL4. Gliotactin was immunoprecipitated using a mAb to Gliotactin, and the western blot simultaneously probed with mAbs to Gliotactin (Gli) and phosphotyrosine (pY). A phosphotyrosine-positive band co-migrated with GliWT. (**B**) GliWT, GliDD and GliFF expression under the control of daughterless–GAL4 in a Gliotactin-null background. Western blots of larval extracts were probed with antibodies to Gliotactin and actin, respectively. Daughterless–GAL4 (da) was used as a wild-type control. Endogenous Gliotactin had degradation products in the control lane comparable to those of GliWT and GliDD larval extracts. GliFF larval extracts had no degradation products. (**C**) Gliotactin can be phosphorylated at tyrosine residues in vitro. A Src kinase assay was employed using a Src–GST fusion paired with the C-terminal domain of Gliotactin, either GliWT or GliFF. Significant tyrosine phosphorylation was detected only for GliWT and Src itself (arrows) in the presence of Src. Neither the GliFF nor the control showed any tyrosine phosphorylation.

Overexpression of Gliotactin results in mislocalization and increased tyrosine phosphorylation

The control of Gliotactin endocytosis by tyrosine phosphorylation suggests that epithelial cells have a mechanism to regulate Gliotactin protein levels. Therefore, we wanted to test the effects of excessive levels of Gliotactin and overexpressed each of the Gliotactin transgenes (GliWT, GliDD and GliFF) in wild-type wing discs using apterous–GAL4 (ap–GAL4). Throughout the overexpression studies, we observed similar phenotypes at both 25°C and 29°C; however, to increase the penetrance, we performed all the experiments at higher temperatures (29°C). The efficiency of GAL4 increases at 29°C, with a corresponding increase in the levels of UAS-Gli expression (supplementary material Fig. S4).

Similar to our rescue experiments, two different insertions were used for each transgene to ensure that the differences in result between GliWT, GliDD and GliFF are not due to differential expression levels. We then analyzed the distribution and subcellular localization of Gliotactin after overexpression in the presence of endogenous Gliotactin. As a control, we overexpressed the membrane protein mCD8GFP using the apterous–GAL4 driver. The mCD8GFP was localized to the cell membrane, and no defects or abnormalities were detected in these wing discs (Fig. 3A).

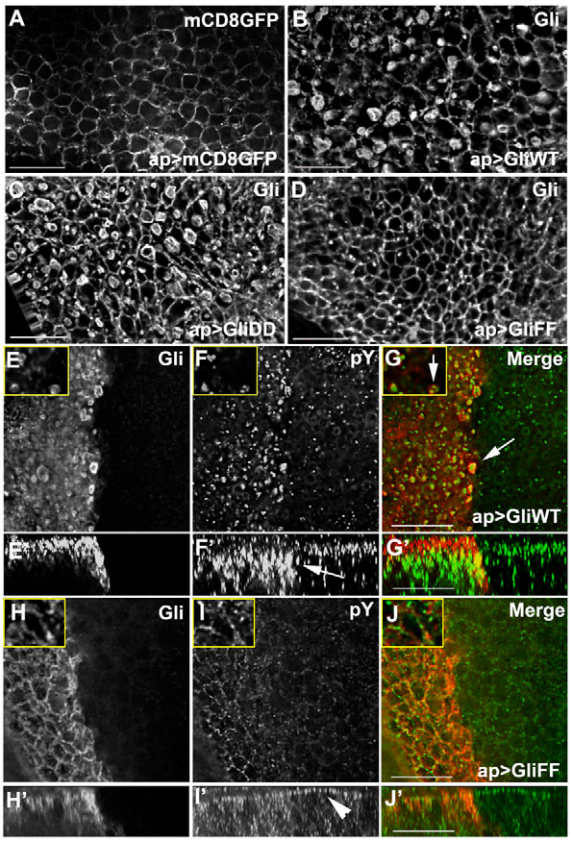

Fig. 3. Overexpression of Gliotactin results in increased tyrosine phosphorylation and endocytosis. In all panels, apterous–GAL4 (ap>) was used to drive expression in wild-type wing imaginal discs. (**A**) ap>mCD8-GFP wing disc, a control disc in which no mCD8GFP was found in intracellular vesicles. (**B–D**) ap>GliWT, GliDD- and GliFF-expressing wing discs, respectively. Gliotactin was detected in intracellular vesicles in all three cases; however, GliDD had the greatest degree of intracellular vesicles and GliFF had very little. (**E–G**) ap>GliWT wing disc, immunolabeled for Gli (red) and phosphoTyr (green). PhosphoTyr levels were enhanced in the dorsal compartment expressing high levels of Gliotactin. High-magnification inserts (digitally scaled by 100%) show phosphoTyr associated with Gliotactin vesicles (arrows). (E′–G′) Side projections of the corresponding panels showing the basolateral spread of both GliWT and phosphoTyr (arrow). (**H–J**) ap>GliFF wing disc, immunolabeled for Gli (red) and phosphoTyr (green). PhosphoTyr levels were only slightly increased in the dorsal compartment. (H′–J′) Side projections of the corresponding panels. The normal localization of phosphoTyr at the adherens junctions is indicated (arrowhead). All enface panels represent a single *Z* slice. Scale bars: 15 µm.

However, in wing discs expressing elevated levels of GliWT, GliDD or GliFF, Gliotactin localization was not restricted to the tricellular corners and was found throughout the entire SJ domain (Fig. 3B–D). Side projections of Gliotactin-overexpressing cells revealed the spread of Gliotactin in the basolateral membrane as well (Fig. 3E′,G′). In addition, a large quantity of Gliotactin was found in intracellular vesicles within the overexpressing cells. GliWT and GliDD had high numbers of internal vesicles, whereas very few Gliotactin-containing intracellular vesicles were detected in GliFF-overexpressing cells (Fig. 3D).

In our analysis of Gliotactin phosphorylation, we were unable to detect colocalization of phosphoTyr with endogenous Gliotactin in wild-type imaginal discs. However, when Gliotactin was overexpressed in the wing imaginal disc using apterous–GAL4, we observed colocalization of phosphoTyr and Gliotactin (Fig. 3E–G). In particular, the large intracellular vesicles were positive for both Gliotactin and phosphoTyr (Fig. 3G, arrows). In these discs, the phosphoTyr immunolabeling was increased and spread basolaterally, below its normal localization at the adherens junction (Fig. 3F′, arrows). To determine whether the increase in phosphoTyr expression was due to the overexpression of Gliotactin, we analyzed discs overexpressing GliFF using apterous–GAL4 (Fig. 3H–J). In these cells, there was only a small increase in phosphoTyr immunolabeling in the GliFF-overexpressing cells. It is important to note that Gliotactin functions as a dimer or oligomer (Venema et al., 2004). As such, it is likely that the small increase in phosphoTyr observed with GliFF was due to the formation of dimers between GliFF and the endogenous Gliotactin.

Overexpression of Gliotactin results in excessive endocytosis and degradation

We then investigated the nature of the Gliotactin vesicles to find out whether they are endosomal or trafficking vesicles. Our immunolabeling data showed no association of Gliotactin vesicles with either the Golgi apparatus or endoplasmic reticulum (supplementary material Fig. S3D–F). Immunolabeling for the early endosomal marker EEA1, however, showed significant upregulation where high levels of Gliotactin were expressed (Fig. 4A–C).

Next, we investigated whether intracellular Gliotactin vesicles were ubiquitinylated as ubiquitylation plays an important role in endocytosis, recycling and targeting of proteins for degradation (Dupre et al., 2001; Katzmann et al., 2001; Piper and Luzio, 2007; Purdy and Russell, 2007; Raiborg et al., 2002). Immunolabeling with an antibody against ubiquitin showed colabeling with internalized Gliotactin, suggesting that ubiquitylation is a part of the process of Gliotactin internalization (Fig. 4D–F). Similarly the endosomal marker Hrs and lysosomal protein LAMP1 also showed colabeling with Gliotactin-containing vesicles (Fig. 4G–I; supplementary material Fig. S3G–I). The different Gliotactin transgenes suggest that these processes are dependent on the conserved tyrosine residues. GliDD overexpression resulted in a greater number of endocytic vesicles, many of which were colabeled by antibodies against LAMP1 and Gliotactin (Fig. 4J–L). GliFF had reduced levels of endocytic vesicles and little to no LAMP1 labeling (supplementary material Fig. S3J–L). The small degree of internalization observed with GliFF is again likely due to dimer or oligomer formation with the endogenous Gliotactin. Together, these data suggest that tyrosine phosphorylation of Gliotactin is necessary for endocytosis and targeting to lysosomes for subsequent degradation.

High levels of Gliotactin lead to cell delamination, migration and death

The controlled regulation of Gliotactin suggests that excessive levels of this protein might be deleterious to the cell. Therefore, we assayed overexpression of Gliotactin in the wing imaginal disc for changes in cell morphology and cell death. Using apterous–GAL4 to drive the expression of GliWT or GliFF in the presence of endogenous Gliotactin resulted in delamination of the columnar epithelial cells (Fig. 5B,D). We also observed that these cells had crossed from the apterous expression boundary and invaded the ventral compartment of the disc (Fig. 5B,D, arrow). These phenotypes were dose dependent, showing the maximum

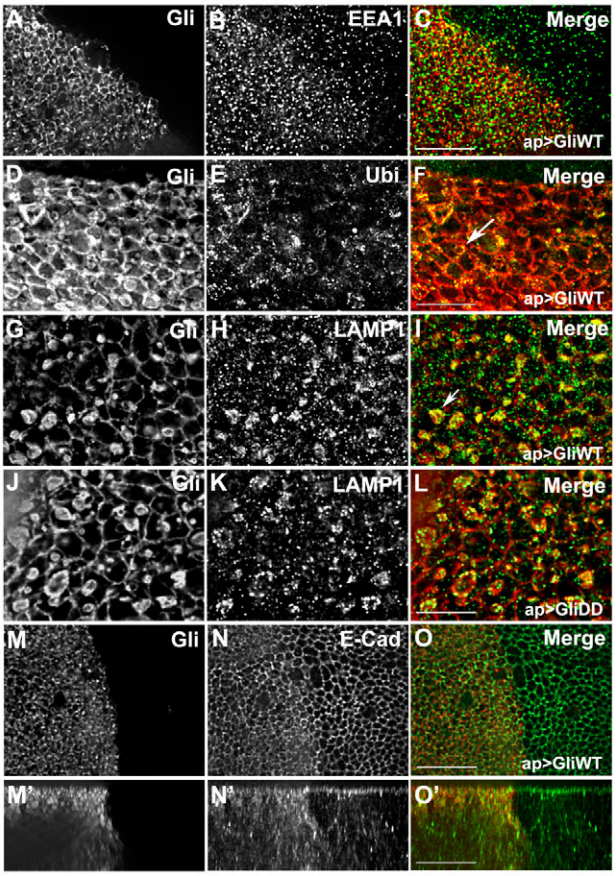

Fig. 4. Overexpression of Gliotactin results in excessive endocytosis and degradation. In all panels, apterous–GAL4 (ap>) was used to drive expression in wild-type wing imaginal discs. (**A–C**) ap>GliWT wing disc, immunolabeled for the early endosomal marker EEA1 (green) and Gli (red) shows an increase in the level of EEA1 at the dorsal compartment. (**D–F**) ap>GliWT wing disc, immunolabeled for Ubiquitin (green) and Gli (red) shows colocalization of Ubiquitin with Gliotactin vesicles (arrow in F). (**G–I**) ap>GliWT wing disc, immunolabeled for the lysosomal marker LAMP1 (green) and Gli (red) shows accumulation of LAMP1 with large Gliotactin vesicles (arrow in I). (**J–L**) ap>GliDD wing disc, immunolabeled for LAMP1 (green) and Gli (red) shows that the large and more numerous vesicles in these cells are also positive for LAMP1. (**M–O**) ap>GliWT wing disc, immunolabeled for E-cadherin (E-cad: green) and Gli (red). Enface view with apterous–GAL4 expression in the dorsal (left) compartment. (M′–O′) The corresponding side projections. Each enface panel represents a single *Z* slice. Scale bars: 15 μm.

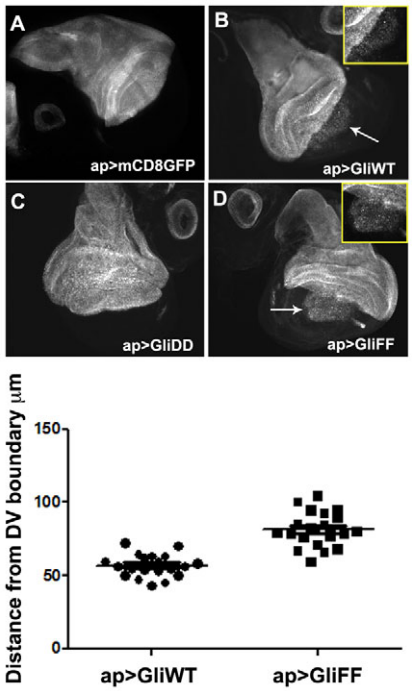

Fig. 5. High levels of Gliotactin cause cell migration from the dorsal to ventral compartments. In all panels, apterous–GAL4 (ap>) was used to drive expression in wild-type wing imaginal discs. (**A**) ap>mCD8GFP wing disc, no GFP labeled cells have crossed the dorsoventral (D–V) boundary and invaded the ventral wild-type compartment. (**B–D**) ap>GliWT, GliDD and GliFF wing discs, immunolabeled for Gliotactin. GliWT and GliFF have a greater degree of cell migration (arrow in B and D), compared with GliDD (C), where no cell migration is seen. In addition, extra folds are apparent in the Gliotactin-overexpressing area for all three transgenes. Inserts in B and D highlight the extent of cell migration. Statistical analysis (lower graphic) of ap>GliWT and ap>GliFF discs showed a significant difference in the distance of migrating cells from the D–V boundary between these two transgenes (n=20 discs, P<0.0002).

penetrance at 29°C, with observable, but weaker, phenotypes at 25°C.

The delamination of Gliotactin-overexpressing cells was not due to disruption of the adherens junctions. The localization of DE-cadherin to the adherens junctions was not affected (Fig. 4M–O) and no other polarity defects were observed. For instance, immunolabeling for the SJ protein Coracle showed no effect (data not shown). Therefore the polarity of cells was not affected in the presence of high levels of Gliotactin. This effect was also specific to Gliotactin as overexpression of other SJ proteins had no effect on cell polarity (Schulte et al., 2006) and no effect on cell survival. For instance, overexpression of Dlg (supplementary material Fig. S5) or NrxIV (data not shown) using apterous–GAL4 did not result in cell delamination or cell death.

If delamination and migration result from the increased presence of Gliotactin in the plasma membrane, the GliFF mutation would be expected to have the greatest effect. To test this, we measured the distance that migrating cells had traveled from the dorsal–ventral boundary of apterous expression into the ventral compartment (Fig. 5). In GliFF-overexpressing discs, migrating cells had traveled a significantly longer distance in comparison with those overexpressing GliWT (Fig. 5B) (n=20 discs). Interestingly, unlike GliWT and GliFF, GliDD overexpression did not result in any cell delamination or migration phenotypes (Fig. 5C) (n=20 discs). These observations suggest that the presence of high levels of Gliotactin throughout the SJ domain might lead to signaling and the activation of apoptotic signals. By contrast, GliDD, which presumably mimics a steady state of tyrosine phosphorylation, is rapidly endocytosed and becomes degraded by lysosomes. The rapid endocytosis and degradation of GliDD might prevent the activation of apoptotic signals.

To test whether the migrating cells are in the process of elimination and death, we immunolabeled wing discs overexpressing each transgene for cleaved Caspase-3, the activated form of the effector caspase in apoptotic cells (Yu et al., 2002). For both GliWT and GliFF, activated Caspase-3 immunolabeling was concentrated in the wing pouch (Fig. 6F,N), corresponding to the

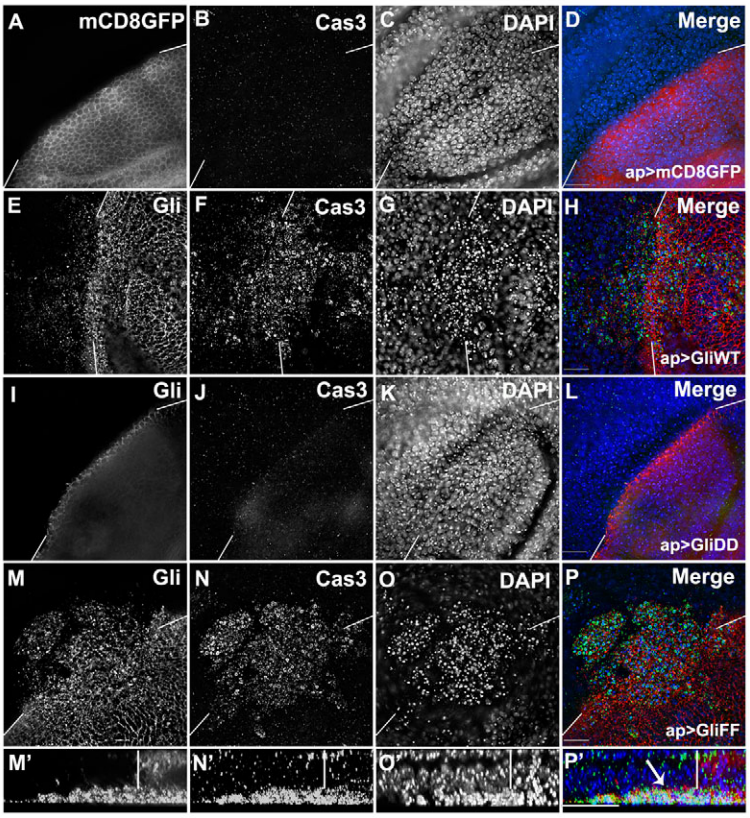

Fig. 6. High levels of Gliotactin causes cell delamination, migration and apoptosis. In all panels, apterous–GAL4 (ap>) was used to drive expression in wild-type wing imaginal discs. (**A–D**) ap>mCD8–GFP wing disc, immunolabeled for GFP (red), activated Caspase-3 (green) and DAPI (blue) showed an intact D–V boundary, and no cell death is detected in these discs. (**E–H**) ap>GliWT wing disc, immunolabeled for Gli (red), activated Caspase-3 (green) and DAPI (blue). At the basal side of the columnar epithelia, activated Caspase-3 was detected in the dorsal compartment close to the D–V boundary as well as in the ventral compartment. DAPI immunolabeling revealed multiple pyknotic nuclei corresponding to the caspase-3-positive cells. (**I–L**) ap>GliDD wing disc, immunolabeled for Gli (red), activated Caspase-3 (green) and DAPI (blue). At the basal side of the columnar epithelia, no cell migration and no apoptosis was detected. (**M–P**) ap>GliFF wing disc, immunolabeled for Gli (red), activated Caspase-3 (green) and DAPI (blue). The greatest degree of cell death was observed as the caspase-3 and DAPI immunolabeling showed an enhanced number of apoptotic cells, with pyknotic nuclei in the basal side of the epithelia. (M′–P′) Side projections of M–P. The apoptotic cells, which are Caspase-3 positive with pyknotic nuclei, have delaminated, fallen below the plane of the epithelia and traveled along the basal membrane (arrow in P′). In all panels, lines indicate the D–V boundary, with the dorsal side to the right. All enface panels were imaged at the most basal level of the columnar epithelia to visualize the delaminated cells. Each panel represents a single *Z* slice. Scale bars: 40 μm.

area of delaminated and migrating cells on the basal side of the epithelium. Colabeling with the nuclear marker DAPI showed that the cells contain pyknotic nuclei, which is a hallmark of apoptosis (Fig. 6G,O). A side projection of the wing discs shows that the delaminated cells were below the plane of the epithelium and travelled along the basal membrane (Fig. 6M′–P′). GliDD overexpression, however, resulted in little or no cell death or delamination (Fig. 6I–L). These results suggest that the levels of Gliotactin are regulated in order to maintain the integrity of epithelial cells. The reduced amount of cell death in GliDD-overexpressing cells also indicates that mimicking tyrosine phosphorylation of Gliotactin likely accelerates the rate of endocytosis and speeds up the removal of excess Gliotactin from the cell membrane.

The preceding experiment tested the effect of overexpression of the different Gliotactin transgenes in the presence of endogenous Gliotactin. Given the ability of Gliotactin to form dimers or oligomers, we wanted to test the effect of each transgene alone in a *Gli* null background. Expression of GliWT and GliDD transgenes, using daughterless–GAL4, in $Gli^{\Delta 45}$ mutant discs, resulted in delaminated cells that were positive for activated Caspase-3 plus contained pyknotic nuclei (supplementary material Fig. S6). These results suggest that, given its extensive endocytosis, the expression of GliDD was not sufficient to fully rescue the cell lethality observed in cells lacking Gliotactin (Venema et al., 2004) (K. Charish, personal communication). Conversely, the spread of GliWT or GliDD beyond the TCJ in these cells might be deleterious, similar to the situation for overexpression experiments. Surprisingly, the GliFF transgene, when expressed in the absence of endogenous Gliotactin, had no evidence of activated Caspase-3 or pyknotic nuclei (supplementary material Fig. S6). These results suggest that, in the absence of endogenous Gliotactin, the lack of endocytosis of GliFF is not deleterious. Collectively, these data suggest that, when overexpressed in a wild-type disc, GliFF blocks the endocytosis of endogenous Gliotactin, and the resulting retention and persistence of wild-type, phosphorylated Gliotactin in the plasma membrane results in cell death.

High levels of Gliotactin increases cell proliferation

In addition to apoptosis, overexpression of Gliotactin in wing discs also resulted in ectopic folds. In order to investigate further these extra folds, we checked whether the ectopic folds were a result of increased cell proliferation. Immunolabeling with phospho-histone3, which labels mitotic cells (Tapia et al., 2006), showed a significant increase in the number of dividing cells in the apterous–GAL4 (dorsal) compartment of the wing disc (Fig. 7A–L). Statistical analysis for the different transgenes revealed that the overexpression of each in the presence of endogenous Gliotactin increased cell proliferation. Of note, GliFF had a higher ratio of cell proliferation compared with GliWT and GliDD, both of which showed similar levels of increased cell division (Fig. 7M–P). These observations suggest that the comparatively higher level of GliFF at the cell membrane leads to increased cell proliferation possibly through the retention of endogenous Gliotactin. An alternative possibility is that the increased number of apoptotic cells in GliFF-expressing discs send proliferation signals to the neighboring cell to compensate for cell loss and to maintain tissue homeostasis, a process known as compensatory proliferation (Fan and Bergmann, 2008).

Overproliferation, cell migration and death resulting from Gli overexpression is mediated by *Drosophila* JNK

One of the major signaling pathways involved in apoptosis, cell proliferation and motility is the Stress-activated Jun N-terminal

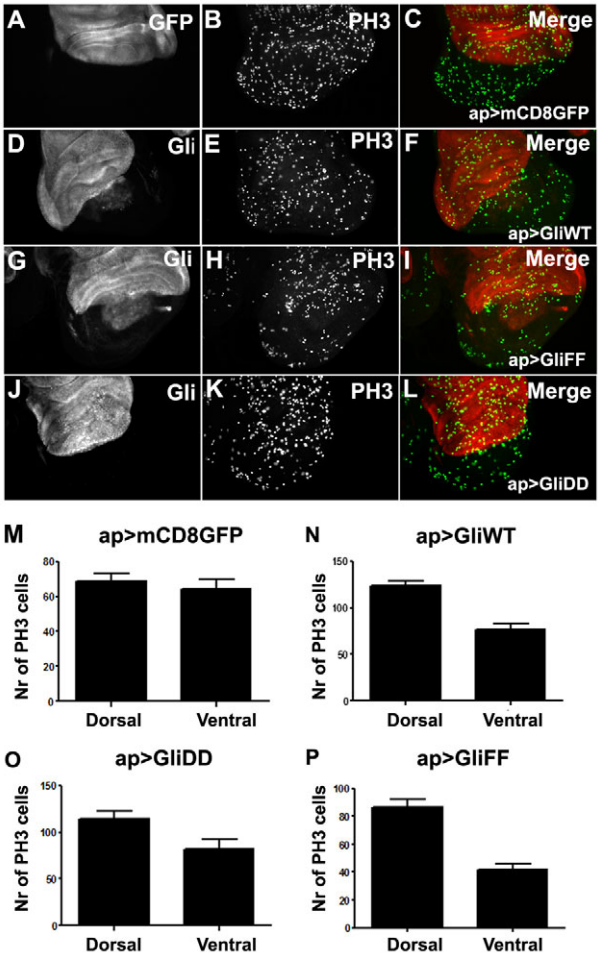

Fig. 7. High levels of Gliotactin cause an increase in mitotic cell division. In all panels, apterous–GAL4 (ap>) was used to drive expression in wild-type wing imaginal discs. (**A–C**) ap>mCD8GFP wing disc, labeled with mCD8GFP (red) and the mitotic marker phospho-histone-3 (PH3; green). In this control, there was no significant difference in number of PH3 cells between ventral and dorsal compartments of the wing pouch. (**D–F**) ap>GliWT wing disc, immunolabeled for Gli (red) and PH3 (green). There were more PH3-positive cells in the dorsal compartment of the wing pouch, where high levels of Gliotactin were present. (**G–I**) ap>GliFF wing disc immunolabeled for Gli (red) and PH3 (green). A higher number of PH3-positive cells were observed in the dorsal area of the wing pouch. (**J–L**) ap>GliDD wing disc immunolabeled for Gli (red) and PH3 (green). An increased number of mitotic cells were observed in the dorsal compartment. (**M–P**) Statistical analysis of cell proliferation in dorsal and ventral compartments for each of GliWT, GliDD and GliFF showed a significant increase in cell proliferation in the dorsal compartment compared with that of the ventral compartment. Bars represent the standard error. ap>mCD8GFP: n=10 discs, P=0.4160; ap>GliWT: n=10 discs, P<0.0001; ap>GliDD: n=10 discs, P=0.0002; ap>GliFF: n=10 discs, P<0.0001.

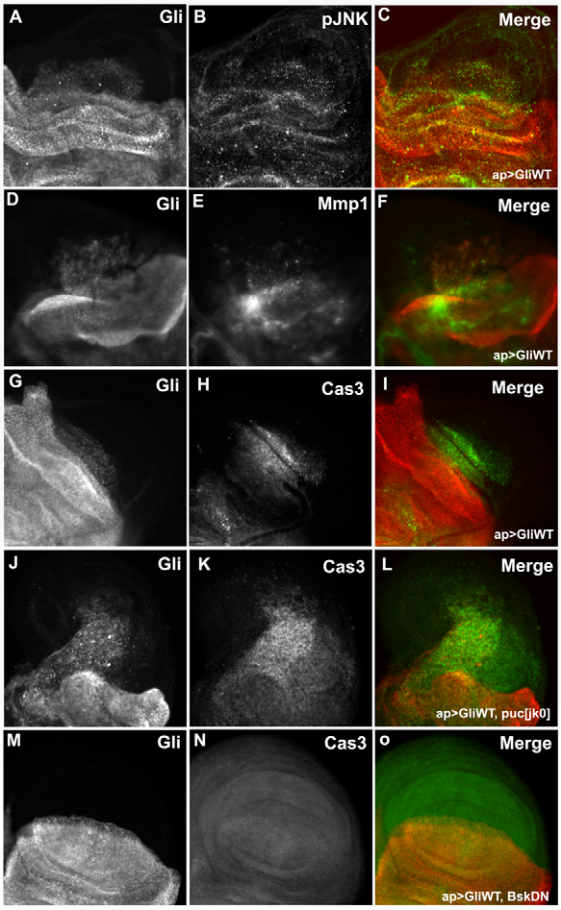

Fig. 8. The cell migration and apoptosis caused by Gliotactin overexpression requires JNK. In all panels, apterous–GAL4 (ap>) was used to drive expression in wild-type wing imaginal discs. (**A–C**) ap>GliWT wing disc, immunolabeled for Gliotactin (red) and phospho-JNK (pJNK; green). Elevated levels of pJNK were detected in the dorsal compartment as well as in the migrating apoptotic cells. (**D–F**) ap>GliWT wing discs, immunolabeled for Gliotactin (red) and a known JNK-induced protein, Mmp1 (green). More Mmp1 is observed in the Gliotactin-overexpressing compartment, especially at the D–V boundary as well as in the migrating cells. (**G–I**) ap>GliWT wing discs, immunolabeled for Gli (red) and activated caspase-3 (green). Migrating cells contain high levels of activated Caspase-3. (**J–L**) ap>GliWT in a puc^{jk0}-heterozygous wing disc, immunolabeled for Gli (red) and activated caspase-3 (green). Reducing the level of the JNK phosphatase Puckered enhanced the migratory behavior and apoptosis of Gliotactin-overexpressing cells. (**M–O**) ap>BskDN, GliWT wing disc, immunolabeled for Gli (red) and activated caspase-3 (green). Coexpression of a dominant-negative form of JNK, Basket (BskDN), with GliWT completely suppressed cell migration and apoptosis. Neither activated caspase-3 nor cell migration was detected, and disc morphology was completely normal. Gliotactin was still detected within intracellular vesicles, as endocytosis was not blocked. The gain on the Caspase-3 image was increased to emphasize the lack of immunolabeling.

kinase JNK (Martin-Blanco et al., 2000; Mattila et al., 2005; McEwen and Peifer, 2005; Perez-Garijo et al., 2009; Ryoo et al., 2004). To test whether JNK is activated downstream of Gliotactin, we looked to see whether JNK signaling was increased when Gliotactin is overexpressed. Immunolabeling with an antibody against phosphoJNK, which detects the activated form of JNK, revealed increased phosphoJNK in the dorsal compartment when GliWT was driven with apterous–GAL4 (Fig. 8A–C). A known target of JNK signaling is *Mmp1* (encoding Matrix metalloproteinase 1) (Uhlirova and Bohmann, 2006), which enhances cell migration by degrading the extracellular matrix (McCawley and Matrisian, 2000; Page-McCaw et al., 2003). Immunolabeling showed increased Mmp1 in the dorsal compartment and in the migrating cells (Fig. 8D–F). Finally, we tested the effect of reducing puckered (*puc*), a phosphatase that negatively regulates JNK (Martin-Blanco et al., 1998). The *puc*

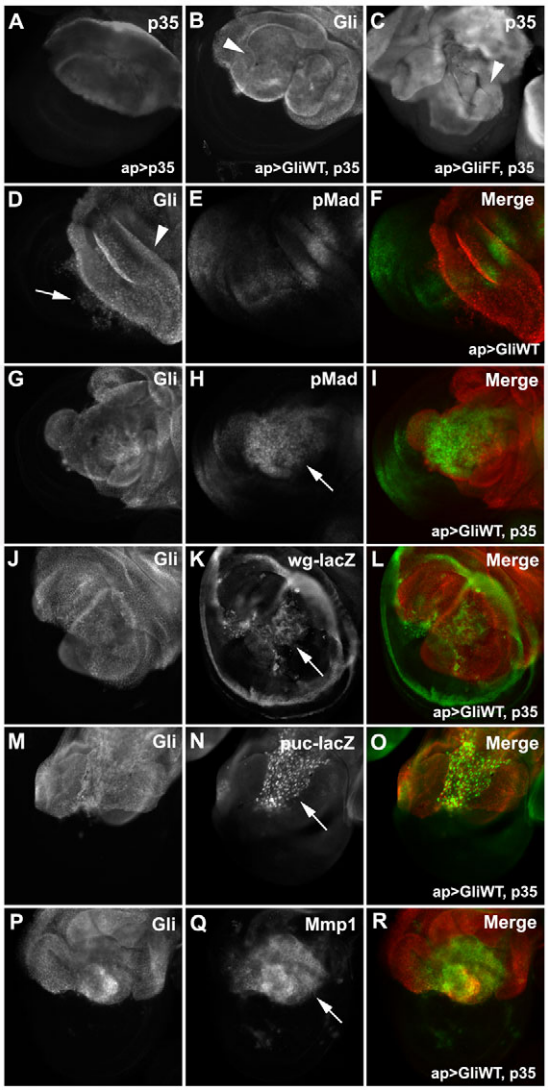

Fig. 9. Blocking apoptosis with p35 in Gliotactin-overexpressing wing imaginal discs results in overgrowth. In all panels, apterous–GAL4 (ap>) was used to drive expression in wild-type wing imaginal discs. (**A**) ap>p35 wing disc, immunolabeled for p35. No abnormality in the morphology of the discs was seen. (**B**) ap>GliWT, p35 wing disc, immunolabeled for Gli. p35 blocked the cell migration but also caused overgrowth and ectopic folds (arrowhead) in the dorsal compartment. (**C**) ap>GliFF, p35 wing disc, immunolabeled for p35. p35 not only blocked cell migration but also resulted in excessive overgrowth and ectopic folds (arrowhead) compared with coexpression with GliWT. (**D–F**) ap>GliWT wing disc, immunolabeled for Gli (red) and phosphoMad (pMad; green). Many cells have left the dorsal compartment and entered the ventral region (arrow). In addition, extra folds were apparent in the Gliotactin-overexpressing area (arrowhead). Gliotactin overexpression alone had no effect on the normal pattern of phosphoMad expression. (**G–I**) ap>GliWT, p35 wing disc, immunolabeled for Gli (red) and pMad (green). The domain of pMad expression was much broader in the dorsal compartment, especially in the wing pouch (arrow), correlating to the region of greatest cell death. (**J–L**) ap>GliWT, p35 wing disc expressing the wingless–lacZ marker, immunolabeled for β-Galactosidase (wg–lacZ; green) and Gli (red). Wingless (wg–lacZ) is ectopically induced in the dorsal compartment of the wing pouch (arrow). (**M–O**) ap>GliWT, p35 wing discs expressing the JNK reporter puckered–lacZ, immunolabeled for β-Galactosidase (puc–lacZ; green) and Gli (red). A significant amount of lacZ was found in the dorsal compartment (arrow), where high levels of Gli and p35 were present. (**P–R**) ap>GliWT, p35 wing discs, immunolabeled for Mmp1 (green) and Gli (red). Mmp1 was ectopically induced in the dorsal compartment, especially in the wing pouch (arrow).

allele when heterozygous effectively increases JNK activity and enhanced the migratory behavior of the Gliotactin-overexpressing cells as well as the associated cell death (Fig. 8J–L), providing further evidence in support of JNK signaling in this process.

Next we asked whether inhibition of JNK signaling is sufficient to block the cell migration and death in the Gliotactin-overexpressing cells. In order to address this question, we coexpressed a dominant-negative form of the *Drosophila* JNK, basket (Bsk^{DN}) with GliWT under the control of apterous–GAL4. Strikingly, inhibition of JNK signaling by expression of Bsk^{DN} completely blocked the invasiveness as well as the cell death caused by overexpression of Gliotactin (Fig. 8M–O). These results suggest that high levels of Gliotactin lead to activation of the JNK pathway. The end result is an increase in mitotic cell division, cell delamination, migration and apoptosis.

Blocking apoptosis with p35 in Gliotactin-overexpressing wing discs results in overgrowth

Given the apoptosis of those cells overexpressing GliWT and GliFF, we wanted to determine the consequences of blocking apoptosis using the baculovirus caspase inhibitor p35 (Hay et al., 1994). Expression of p35 alone using apterous–GAL4 did not affect the normal development of wing imaginal discs (Fig. 9A). However, blocking apoptosis with p35 in wing discs expressing high levels of Gliotactin resulted in overgrowth of the apterous–GAL4 compartment (Fig. 9B). Specifically, we observed increased folding and an absence of cell migration into the ventral compartment. Blocking apoptosis in GliFF-overexpressing discs (Fig. 9C) resulted in dramatically enhanced overgrowth compared with GliWT coexpressed with p35 (Fig. 9B). The more severe overgrowth phenotype in those cells expressing both GliFF and p35 could be due to a lack of endocytosis and the persistence of Gliotactin-mediated signaling at the plasma membrane. Conversely, the greater number of apoptotic cells observed in the GliFF-overexpressing discs could contribute to a higher level of compensatory proliferation. Blocking apoptosis with p35 has been shown to keep the dying cells in an ‘undead’ state such that these cells continuously send compensatory proliferation signals to the neighboring cells, resulting in tissue overgrowth (Martin et al., 2008).

Overgrowth after Gli overexpression is mediated by JNK signaling

Previous studies have reported a role for *Drosophila* JNK in compensatory proliferation (Fan and Bergmann, 2008; Perez-Garijo et al., 2004; Ryoo et al., 2004). JNK is the main regulator of compensatory proliferation, and it induces the activity of Protein wingless (Wg) and Protein decapentaplegic (Dpp) (Perez-Garijo et al., 2009). The ectopic expression of these mitogens when apoptosis is blocked results in overgrowth. Given the role of JNK signaling downstream of Gliotactin, we checked for ectopic Dpp, Wg or JNK activation in wing discs expressing both GliWT and p35 under the control of apterous–GAL4 (Fig. 9). Immunolabeling with an antibody against phosphoMad, which detects the activated form of Mad, a target of Dpp (Teleman and Cohen, 2000), showed ectopic expression in the dorsal compartment overexpressing

Gliotactin and p35 (Fig. 9G–I). Similar observations were made with wingless–lacZ and puckered–lacZ reporters, which reflect the activation of endogenous Wg and JNK, respectively (Fig. 9J–O) (McEwen and Peifer, 2005). In addition, the JNK target Mmp1 also showed ectopic activation in the dorsal compartment overexpressing Gliotactin and p35 (Fig. 9P–R). These observations further support the view that JNK signaling and its targets are activated by overexpression of Gliotactin. The dramatic overgrowth seen with GliWT and GliFF in the presence of p35 suggests that JNK might also be initiating the compensatory proliferation pathway in these cells.

Discussion

Tricellular junctions, in spite of their importance in the formation and maintenance of SJs and the establishment of permeability barriers, have received very little attention. Currently, in *Drosophila*, Gliotactin is the only protein uniquely located to the TCJ complex (Schulte et al., 2003). However, little is known about the localization, interaction with other SJ components and the function of individual domains of Gliotactin. Here, we demonstrate that the two conserved tyrosine residues of Gliotactin, Y766 and Y790, are necessary for the endocytosis and degradation of Gliotactin. Mutation of these residues to phenylalanine blocks the endocytosis of Gliotactin and its subsequent degradation. Conversely, mutation of these residues to aspartate increases endocytosis and promotes degradation.

Phosphorylation by tyrosine kinases and subsequent endocytosis is a key mechanism for downregulation of signaling molecules (Chen et al., 2007) and adherens junctions (Behrens et al., 1993). However, little is known about the regulation of junctional complexes that form at the septate or tricellular permeability barrier. Our data suggest that tyrosine phosphorylation, endocytosis and degradation might be a mechanism to localize and restrict Gliotactin to the TCJ. Blocking endocytosis with dominant-negative Rab5 expression resulted in the spread of Gliotactin beyond the TCJ into the bicellular SJ. This points to the existence of an endocytic mechanism to remove excess Gliotactin from the SJ domain.

Why is there a mechanism to remove excess Gliotactin? Our previous work indicated that high levels of Gliotactin in the bicellular SJ resulted in Gliotactin binding to other SJ components such as Neurexin IV (NrxIV) and reduced the level of Dlg (Schulte et al., 2006). One possible explanation could be that the interaction of Gliotactin with SJ components might block the normal interactions of these components and disrupt cell polarity or junction assembly, resulting in cell death. However, overexpression of Gliotactin did not lead to changes in cell polarity or loss of cell adhesion. Another possibility is that overexpression of SJ proteins in general might result in cell death. However, the overexpression of Dlg or NrxIV had no effect on cell viability. Alternatively, the spread of Gliotactin into the SJ domain might trigger a signaling cascade that is regulated by the rapid endocytosis of Gliotactin. In support of this, GliDD, which mimics phosphorylation of Gli, when overexpressed resulted in more endocytic vesicles and induced little or no cell delamination or apoptosis. The increased delamination and cell death observed with the overexpression of GliFF supports the idea that phosphorylation of the tyrosine residues is part of a mechanism to remove Gliotactin rapidly from bicellular SJs. This also suggests that the increased presence of Gliotactin within the SJ or the plasma membrane triggers a cell signal that needs to be controlled. The contrasting results we observed between the expression of GliFF alone in a null background compared with expression in the presence of endogenous Gliotactin point to a signaling mechanism that is controlled by one or both of the conserved tyrosine residues in Gliotactin. Gliotactin, like other members of the neuroligin family, forms dimers or oligomers (Venema et al., 2004). Thus, we suggest that overexpression of GliFF blocks the endocytosis of endogenous Gliotactin proteins, resulting in persistent Gliotactin signaling in the bicellular SJ domain through the phosphoTyr domains.

A strong candidate for a signaling pathway downstream of ectopic Gliotactin is the JNK pathway. Overexpression of Gliotactin resulted in the upregulation of phospho-JNK and JNK targets such as Mmp1. Blocking JNK signaling completely suppressed the cell migration and death induced by overexpression of Gliotactin. Conversely, increasing JNK activity enhanced the overexpression phenotypes of Gliotactin, including an increase in cell death and migration.

One of our interesting findings was the increase in number of mitotic cells and the generation of ectopic folds in the presence of high levels of Gliotactin. The enhanced proliferation in the presence of excess Gliotactin could reflect a signaling pathway occurring downstream of Gliotactin in mediating cell proliferation. Alternatively, the cell death associated with ectopic Gliotactin could stimulate compensatory proliferation, which is also under the control of the JNK pathway (Perez-Garijo et al., 2009).

Coexpression of Gliotactin and p35 to block apoptosis resulted in enhanced overgrowth, especially in the case of GliFF. It has been shown previously that, if apoptosis is blocked by p35, the remaining ‘undead’ cells continue to secrete compensatory proliferating signals to their neighboring cells, resulting in tissue overgrowth (Fan and Bergmann, 2008; Martin et al., 2008). When p35 was coexpressed with Gliotactin, we observed an upregulation of Dpp and Wg signaling, and overall our results mirror the effects downstream of JNK in the compensatory proliferation pathway (McEwen and Peifer, 2005). Therefore, it is likely that the high level and the subsequent spread of Gliotactin away from the TCJ leads to the activation of JNK, resulting in delamination and apoptosis. Downstream of JNK, compensatory proliferation is induced to make up for the loss of imaginal disc cells. It still remains to be investigated how these processes communicate to each other and why the spread of Gliotactin away from the TCJ in the membrane leads to the activation of the JNK pathway.

Materials and Methods

Fly stocks

The following fly strains were used: Gliotactin null alleles, $Gli^{\Delta E2\Delta 45}$ and Gli^{CR2} (Venema et al., 2004), UAS lines including UAS-GliWT, UAS-GliDD, UAS-GliFF (generated below), UAS-mCD8GFP, UAS-Rab5DN, UAS-p35 and $NrxIV^{EP604}$ from the Bloomington stock center, UAS-Bsk^{DN} from the DGRC Kyoto stock center, UAS-DlgGFP from D. Bilder. The daughterless–GAL4 and apterous–GAL4 lines from the Bloomington stock center were used as GAL4 drivers. Puckered–lacZ A251.1F3 from Bloomington stock center and wingless–lacZ were used as reporter lines for *Drosophila* JNK and Wg, respectively. The puc^{jk0} allele, an imprecise excision in *puckered* (Kirchner et al., 2007), and w^{1118}, used as wild type, were from the Bloomington stock center.

Generation of transgenic lines

For generation of different Gliotactin transgenic lines, the N-terminus of Gliotactin (GliNter), the entire extracellular coding sequence and the transmembrane domain was amplified from a Gliotactin cDNA (AE27.41) (Auld et al., 1995) using the following primers: GliNter5 (5′-AGATCTACAGGTGAGAGTTCGCTGCGC-3′) and GliNter3 (5′-GAATTCACTAGTCACATGATGCAGCAGATGACC-3′). Similarly, the C-terminus of Gli (GliCter) was amplified using the following primers: 5′-GGAATTCCGCAATGCCAAGCGCCAATC-3′) and 5′-GTCGAGGGAGTG-CCTCAGACATCCGTATAA-3′, for 5′ end and 3′ ends, respectively. PCR products were then subcloned into the PGEMT vector (Promega) and sequenced for verification. Site-directed mutagenesis was carried out on the GliCter constructs

using the Quik Change Kit (Stratagene). The following primers were employed for generation of different tyrosine residue mutations:

Y790D mutation –
GliY1D1 (5′-CCAGGGATAATATCGACGAGTACCGCGACTCTCC-3′) and
GliY1D2 (5′-GGAGAGTCGCGGTACTCGTCGATATTATCCCTGG-3′);
Y766D mutation –
GliY2D1 (5′-CCAATCGATCGCTTCGATGACGAAGATGTCTTC-3′) and
GliY2D2 (5′-GAAGACATCTTCGTCATCGAAGCGATCCGATTGG-3′);
Y790F mutation –
GliY1F1 (5′-CCAGGGATAATATCTTCGAGTACCGCGACTCTCC-3′) and
GliY1F2 (5′-GGAGAGTCGCCGGTACTCGAAGATATTATCCCTGG-3′);
Y766F mutation –
GliY2F1 (5′-CCAATCGGATCGCTTCTTTGACGAAGATGTCTTC-3′) and
GliY2F2 (5′-GAAGACATCTTCGTCAAAGAAGCGATCCGATTGG-3′).

The resulting plasmids were sequenced for verification, and each individual mutation was then treated with a second round to generate the necessary double mutations GliDD (Y766D, Y790D) and GliFF (Y766F, Y790F).

The two parts of Gliotactin were then subcloned into a modified pUAST vector (pUAS-linker1). GliNter was introduced using the *Bgl*II, *Eco*RI digest to generate pUAS-GliNter, and each GliCter product (WT, DD or FF) was introduced using an *Eco*RI, *Xho*I digest to generate pUAS-GliWT, pUAS-GliDD or pUAS-GliFF, respectively. Each construct was sequenced to verify accuracy and then sent to Genetics Services (Cambridge, MA) for generation of transgenic lines.

Biochemistry

Generation of His-tagged Gliotactin C-terminal constructs

The Gliotactin C-terminal domain with and without the Y766F and Y790F mutations were subcloned from pGEX4T Gliotactin C-terminal constructs into pET28a (Novagen) using *Eco*RI and *Xho*I sites. The final construct was transformed into BL21DE3 pLysS competent cells (Invitrogen). Protein expression was induced using 1 mM IPTG for 45 min, and the cells were lysed in 40 mM imidazole, 300 mM NaCl, 50 mM Tris-HCl pH 8, 1/100 PhosStop (Roche), 1/100 Complete (Roche). His-tagged proteins were purified using Nickel NTA-agarose (Qiagen), eluted with 250 mM imidazole buffer (300 mM NaCl, 50 mM Tris-HCl pH 8) and dialyzed using Slide-A-Lyzer 7000MWCO cassettes (Pierce) into Kinase Buffer (25 mM Tris-HCl pH 7.5, 5 mM β-glycerophosphate, 2 mM DTT, 0.1 mM sodium orthovanadate, 10 mM $MgCl_2$).

Kinase assay

A 50 µl Kinase Reaction [1 µg GliCter in pET28, 1 µg GST–Src (Cell Signaling Technologies), 1× Kinase Buffer, 1 mM ATP] was incubated at 30°C for 1 h. One quarter of this reaction was loaded for SDS-PAGE and western blot analysis.

Immunoprecipitations

Approximately 20 adult flies overexpressing GliWT, GliFF or GliDD with daughterless–GAL4 were homogenized in 20 mM Tris-HCl pH 8, 137 mM NaCl, 10% Glycerol, 1% NP-40, 2 mM EDTA, 1/100 Complete (Roche) and 1/100 PhosStop (Roche). Lysates were spun at 12,000 ***g*** for 10 min at 4°C. Supernatants were added to 20 µl of Protein G agarose (Calbiochem), previously incubated with ~1 µg of mouse anti-Gliotactin IF6.3 antibody (Auld et al., 1995). The beads were washed four times with 20 mM Tris-HCl pH 8, 137 mM NaCl, 10% glycerol, 1% NP-40, 2 mM EDTA and once with PBS, then bound proteins were eluted in loading buffer.

Licor western blot analysis

Samples were run on 10% SDS-PAGE gels then transferred to nitrocellulose membranes. Blots were blocked using 50% Odyssey blocking buffer (LI-COR) diluted in PBS for LI-COR Odyssey fluorescent detection systems. The primary antibodies rabbit anti-Gli 1F6.3 and mouse anti-phosphoTyr 4G10 (a gift from M. Gold) and secondary antibodies goat anti-rabbit IRDye 680, goat anti-mouse IRDye 800, goat anti-mouse IRDye 680 and goat anti-rabbit IRDye 800 were all used at a dilution of 1:20,000 (All IRDye antibodies from Rockland).

ECL western blot analysis of rescued larval extracts

Larval extracts were prepared in loading buffer, run on a 10% SDS-PAGE gel and transferred to nitrocellulose membranes. Blots were blocked in 5% milk buffer and probed with mouse anti-Gli IF6.3 antibody at 1:500. Bands were detected using a HRP-conjugated anti-mouse secondary antibody at 1:10,000 (Jackson Laboratories) and ECL detection (PerkinElmer). The blot was stripped with stripping buffer (Thermo) and probed with a mouse anti-actin antibody at 1:20,000 (ICN Biomedicals).

Immunofluorescence labeling

Wing discs of third-instar larvae were immunolabeled as described previously (Schulte et al., 2006). Primary antibodies and their dilutions were as follows: mouse anti-Gli IF6.3 at 1:200 (Auld et al., 1995), rabbit anti-Gli at 1:300 (Venema et al., 2004), mouse anti-Dlg 4F3 at 1:200 (Parnas et al., 2001), guinea pig anti-Hrs at 1:500 (Lloyd et al., 2002), rabbit anti-EEA1 at 1:200 (Abcam), mouse anti-phosphoTyr (4G10) at 1:200 (a gift from M. Gold), rabbit anti-LAMP1 at 1:300 (Abcam), rat anti-DE-Cadherin at 1:50 (Oda et al., 1994), rabbit anti-activated Caspase-3 (Abcam), mouse anti-Ubiquitin at 1:200 (a gift from I. R. Nabi), rabbit anti-PhosphoH3 at 1:500 (Abcam), rabbit anti-p35 at 1:300 (BIOCARTA), rabbit anti-phosphoJNK at 1:200 (a gift from M. Gold), mouse anti-Mmp1 at 1:100 (Page-McCaw et al., 2003), rabbit anti-phosphoMad at 1:300 (a gift from D. Allan), rabbit anti-βGal (Abcam), mouse anti-Golgi at 1:200 (Calbiochem), rabbit-anti-Calnexin at 1:300 (a gift from I. R. Nabi). The monoclonal antibodies listed from the Developmental Studies Hybridoma Bank were developed under the auspices of the NICHD and maintained by The University of Iowa, Department of Biology. The following secondary antibodies and dilutions were used: goat anti-rabbit Alexa 488 at 1:300, goat anti-mouse Alexa 568 at 1:300, goat anti-rat A647 at 1:300, goat anti-rabbit-A568 at 1:300, goat anti-mouse Alexa 488 at 1:300 (Molecular Probes).

Imaging

Image stacks were collected with a DeltaVision Spectris microscope (Applied Precision), on an Olympus IX70 with a ×60 oil-immersion lens (NA 1.4), using 0.2 µm *Z* sections. The image stacks were deconvolved with SoftWorx (Applied Precision), based on measured point-spread functions from 0.2 µm fluorescent beads (Molecular Probes) mounted in Vectashield. Side projections were created using the SoftWorx program. Images were exported to Photoshop for compilation. For lower magnification, images were collected with a ×20 objective on a Zeiss Axioskop using Northern Eclipse software.

Statistical analysis

The distance travelled by migrating cells from the D–V boundary was measured using the linear tool in Northern Eclipse. Overproliferation was measured for each of the apterous>Gli transgenes, GliWT, GliDD and GliFF as well as for the apterous>mCDGFP discs. For each, comparable areas from the dorsal and ventral compartments of the wing pouch were selected, and the number of objects (PH3 cells) in each was counted digitally using Northern Eclipse software. For statistical analysis, GraphPad Prism software was used to perform a paired *t*-test on the two sets of data to be compared.

We thank Hugo Bellen, Mike Gold, Robert Nabi and Doug Allen for generously providing antibodies; Dave Bilder, the Bloomington and DGRC Stock Centers for fly stocks; and Cal Roskelley for helpful discussions and comments on the manuscript. This study was supported by a grant to V.J.A. from the Canadian Institutes of Health Research.

Supplementary material available online at
http://jcs.biologists.org/cgi/content/full/123/23/4052/DC1

References

Ahmadian, G., Ju, W., Liu, L., Wyszynski, M., Lee, S. H., Dunah, A. W., Taghibiglou, C., Wang, Y., Lu, J., Wong, T. P. et al. (2004). Tyrosine phosphorylation of GluR2 is required for insulin-stimulated AMPA receptor endocytosis and LTD. *EMBO J.* **23**, 1040-1050.

Auld, V. J., Fetter, R. D., Broadie, K. and Goodman, C. S. (1995). Gliotactin, a novel transmembrane protein on peripheral glia, is required to form the blood-nerve barrier in Drosophila. *Cell* **81**, 757-767.

Baumgartner, S., Littleton, J. T., Broadie, K., Bhat, M. A., Harbecke, R., Lengyel, J. A., Chiquet-Ehrismann, R., Prokop, A. and Bellen, H. J. (1996). A Drosophila neurexin is required for septate junction and blood-nerve barrier formation and function. *Cell* **87**, 1059-1068.

Behrens, J., Vakaet, L., Friis, R., Winterhager, E., Van Roy, F., Mareel, M. M. and Birchmeier, W. (1993). Loss of epithelial differentiation and gain of invasiveness correlates with tyrosine phosphorylation of the E-cadherin/beta-catenin complex in cells transformed with a temperature-sensitive v-SRC gene. *J. Cell Biol.* **120**, 757-766.

Brand, A. H. and Perrimon, N. (1993). Targeted gene expression as a means of altering cell fates and generating dominant phenotypes. *Development* **118**, 401-415.

Cantarelli, V. V., Kodama, T., Nijstad, N., Abolghait, S. K., Nada, S., Okada, M., Iida, T. and Honda, T. (2007). Tyrosine phosphorylation controls cortactin binding to two enterohaemorrhagic Escherichia coli effectors: Tir and EspFu/TccP. *Cell. Microbiol.* **9**, 1782-1795.

Chen, W. L., Lin, C. T., Lo, H. F., Lee, J. W., Tu, I. H. and Hu, F. R. (2007). The role of protein tyrosine phosphorylation in the cell-cell interactions, junctional permeability and cell cycle control in post-confluent bovine corneal endothelial cells. *Exp. Eye. Res.* **85**, 259-269.

Cuevas, B. D., Lu, Y., Mao, M., Zhang, J., LaPushin, R., Siminovitch, K. and Mills, G. B. (2001). Tyrosine phosphorylation of p85 relieves its inhibitory activity on phosphatidylinositol 3-kinase. *J. Biol. Chem.* **276**, 27455-27461.

Dupre, S., Volland, C. and Haguenauer-Tsapis, R. (2001). Membrane transport: ubiquitylation in endosomal sorting. *Curr. Biol.* **11**, R932-R934.

Fan, Y. and Bergmann, A. (2008). Apoptosis-induced compensatory proliferation. The Cell is dead. Long live the Cell! *Trends Cell Biol.* **18**, 467-473.

Fehon, R. G., Dawson, I. A. and Artavanis-Tsakonas, S. (1994). A Drosophila homologue of membrane-skeleton protein 4.1 is associated with septate junctions and is encoded by the coracle gene. *Development* **120**, 545-557.

Fristrom, D. K. (1982). Septate junctions in imaginal disks of Drosophila: a model for the redistribution of septa during cell rearrangement. *J. Cell Biol.* **94**, 77-87.
Genova, J. L. and Fehon, R. G. (2003). Neuroglian, Gliotactin, and the Na+/K+ ATPase are essential for septate junction function in Drosophila. *J. Cell Biol.* **161**, 979-989.
Gilbert, M. M. and Auld, V. J. (2005). Evolution of clams (cholinesterase-like adhesion molecules): structure and function during development. *Front. Biosci.* **10**, 2177-2192.
Gilbert, M., Smith, J., Roskams, A. J. and Auld, V. J. (2001). Neuroligin 3 is a vertebrate gliotactin expressed in the olfactory ensheathing glia, a growth-promoting class of macroglia. *Glia* **34**, 151-164.
Hay, B. A., Wolff, T. and Rubin, G. M. (1994). Expression of baculovirus P35 prevents cell death in Drosophila. *Development* **120**, 2121-2129.
Huh, J. R., Guo, M. and Hay, B. A. (2004). Compensatory proliferation induced by cell death in the Drosophila wing disc requires activity of the apical cell death caspase Dronc in a nonapoptotic role. *Curr. Biol.* **14**, 1262-1266.
Ivanov, A. I., Nusrat, A. and Parkos, C. A. (2005). Endocytosis of the apical junctional complex: mechanisms and possible roles in regulation of epithelial barriers. *BioEssays* **27**, 356-365.
Jekely, G. and Rorth, P. (2003). Hrs mediates downregulation of multiple signalling receptors in Drosophila. *EMBO Rep.* **4**, 1163-1168.
Katzmann, D. J., Babst, M. and Emr, S. D. (2001). Ubiquitin-dependent sorting into the multivesicular body pathway requires the function of a conserved endosomal protein sorting complex, ESCRT-I. *Cell* **106**, 145-155.
Kirchner, J., Gross, S., Bennett, D. and Alphey, L. (2007). The nonmuscle myosin phosphatase PP1beta (flapwing) negatively regulates Jun N-terminal kinase in wing imaginal discs of Drosophila. *Genetics* **175**, 1741-1749.
Lloyd, T. E., Atkinson, R., Wu, M. N., Zhou, Y., Pennetta, G. and Bellen, H. J. (2002). Hrs regulates endosome membrane invagination and tyrosine kinase receptor signaling in Drosophila. *Cell* **108**, 261-269.
Marois, E., Mahmoud, A. and Eaton, S. (2006). The endocytic pathway and formation of the Wingless morphogen gradient. *Development* **133**, 307-317.
Martin, F. A., Perez-Garijo, A. and Morata, G. (2008). Apoptosis in Drosophila: compensatory proliferation and undead cells. *Int. J. Dev. Biol.* **53**, 1341-1437.
Martin-Blanco, E., Gampel, A., Ring, J., Virdee, K., Kirov, N., Tolkovsky, A. M. and Martinez-Arias, A. (1998). puckered encodes a phosphatase that mediates a feedback loop regulating JNK activity during dorsal closure in Drosophila. *Genes Dev.* **12**, 557-570.
Martin-Blanco, E., Pastor-Pareja, J. C. and Garcia-Bellido, A. (2000). JNK and decapentaplegic signaling control adhesiveness and cytoskeleton dynamics during thorax closure in Drosophila. *Proc. Natl. Acad. Sci. USA* **97**, 7888-7893.
Mattila, J., Omelyanchuk, L., Kyttala, S., Turunen, H. and Nokkala, S. (2005). Role of Jun N-terminal Kinase (JNK) signaling in the wound healing and regeneration of a Drosophila melanogaster wing imaginal disc. *Int. J. Dev. Biol.* **49**, 391-399.
McCawley, L. J. and Matrisian, L. M. (2000). Matrix metalloproteinases: multifunctional contributors to tumor progression. *Mol. Med. Today* **6**, 149-156.
McEwen, D. G. and Peifer, M. (2005). Puckered, a Drosophila MAPK phosphatase, ensures cell viability by antagonizing JNK-induced apoptosis. *Development* **132**, 3935-3946.
Meyer, T. N., Hunt, J., Schwesinger, C. and Denker, B. M. (2003). Galpha12 regulates epithelial cell junctions through Src tyrosine kinases. *Am. J. Physiol. Cell Physiol.* **285**, C1281-C1293.
Noirot-Timothee, C., Graf, F. and Noirot, C. (1982). The specialization of septate junctions in regions of tricellular junctions. II. Pleated septate junctions. *J. Ultrastruct. Res.* **78**, 152-165.
Oda, H., Uemura, T., Harada, Y., Iwai, Y. and Takeichi, M. (1994). A Drosophila homolog of cadherin associated with armadillo and essential for embryonic cell-cell adhesion. *Dev. Biol.* **165**, 716-726.
Page-McCaw, A., Serano, J., Sante, J. M. and Rubin, G. M. (2003). Drosophila matrix metalloproteinases are required for tissue remodeling, but not embryonic development. *Dev. Cell* **4**, 95-106.
Parnas, D., Haghighi, A. P., Fetter, R. D., Kim, S. W. and Goodman, C. S. (2001). Regulation of postsynaptic structure and protein localization by the Rho-type guanine exchange factor dPix. *Neuron* **32**, 415-424.
Paul, S. M., Ternet, M., Salvaterra, P. M. and Beitel, G. J. (2003). The Na^+/K^+ ATPase is required for septate junction function and epithelial tube-size control in the Drosophila tracheal system. *Development* **130**, 4963-4974.
Perez-Garijo, A., Martin, F. A. and Morata, G. (2004). Caspase inhibition during apoptosis causes abnormal signalling and developmental aberrations in Drosophila. *Development* **131**, 5591-5598.
Perez-Garijo, A., Shlevkov, E. and Morata, G. (2009). The role of Dpp and Wg in compensatory proliferation and in the formation of hyperplastic overgrowths caused by apoptotic cells in the Drosophila wing disc. *Development* **136**, 1169-1177.
Piper, R. C. and Luzio, J. P. (2007). Ubiquitin-dependent sorting of integral membrane proteins for degradation in lysosomes. *Curr. Opin. Cell Biol.* **19**, 459-465.
Purdy, G. E. and Russell, D. G. (2007). Ubiquitin trafficking to the lysosome: keeping the house tidy and getting rid of unwanted guests. *Autophagy* **3**, 399-401.
Raiborg, C. and Stenmark, H. (2009). The ESCRT machinery in endosomal sorting of ubiquitylated membrane proteins. *Nature* **458**, 445-452.
Raiborg, C., Bache, K. G., Gillooly, D. J., Madshus, I. H., Stang, E. and Stenmark, H. (2002). Hrs sorts ubiquitinated proteins into clathrin-coated microdomains of early endosomes. *Nat. Cell Biol.* **4**, 394-398.
Ryoo, H. D., Gorenc, T. and Steller, H. (2004). Apoptotic cells can induce compensatory cell proliferation through the JNK and the Wingless signaling pathways. *Dev. Cell* **7**, 491-501.
Schulte, J., Tepass, U. and Auld, V. J. (2003). Gliotactin, a novel marker of tricellular junctions, is necessary for septate junction development in Drosophila. *J. Cell Biol.* **161**, 991-1000.
Schulte, J., Charish, K., Que, J., Ravn, S., MacKinnon, C. and Auld, V. J. (2006). Gliotactin and Discs large form a protein complex at the tricellular junction of polarized epithelial cells in Drosophila. *J. Cell Sci.* **119**, 4391-4401.
Takeda, H., Nagafuchi, A., Yonemura, S., Tsukita, S., Behrens, J., Birchmeier, W. and Tsukita, S. (1995). V-src kinase shifts the cadherin-based cell adhesion from the strong to the weak state and beta catenin is not required for the shift. *J. Cell Biol.* **131**, 1839-1847.
Tanos, B. and Pendergast, A. M. (2006). Abl tyrosine kinase regulates endocytosis of the epidermal growth factor receptor. *J. Biol. Chem.* **281**, 32714-32723.
Tapia, C., Kutzner, H., Mentzel, T., Savic, S., Baumhoer, D. and Glatz, K. (2006). Two mitosis-specific antibodies, MPM-2 and phosphoHistoneH3 (Ser28), allow rapid and precise determination of mitotic activity. *Am. J. Surg. Pathol.* **30**, 83-89.
Teleman, A. A. and Cohen, S. M. (2000). Dpp gradient formation in the Drosophila wing imaginal disc. *Cell* **103**, 971-980.
Tsukita, S., Furuse, M. and Itoh, M. (2001). Multifunctional strands in tight junctions. *Nat. Rev. Mol. Cell Biol.* **2**, 285-293.
Uhlirova, M. and Bohmann, D. (2006). JNK- and Fos-regulated Mmp1 expression cooperates with Ras to induce invasive tumors in Drosophila. *EMBO J.* **25**, 5294-5304.
Venema, D. R., Zeev-Ben-Mordehai, T. and Auld, V. J. (2004). Transient apical polarization of Gliotactin and Coracle is required for parallel alignment of wing hairs in Drosophila. *Dev. Biol.* **275**, 301-314.
Wucherpfennig, T., Wilsch-Brauninger, M. and Gonzalez-Gaitan, M. (2003). Role of Drosophila Rab5 during endosomal trafficking at the synapse and evoked neurotransmitter release. *J. Cell Biol.* **161**, 609-624.
Yu, S. Y., Yoo, S. J., Yang, L., Zapata, C., Srinivasan, A., Hay, B. A. and Baker, N. E. (2002). A pathway of signals regulating effector and initiator caspases in the developing Drosophila eye. *Development* **129**, 3269-3278.

A

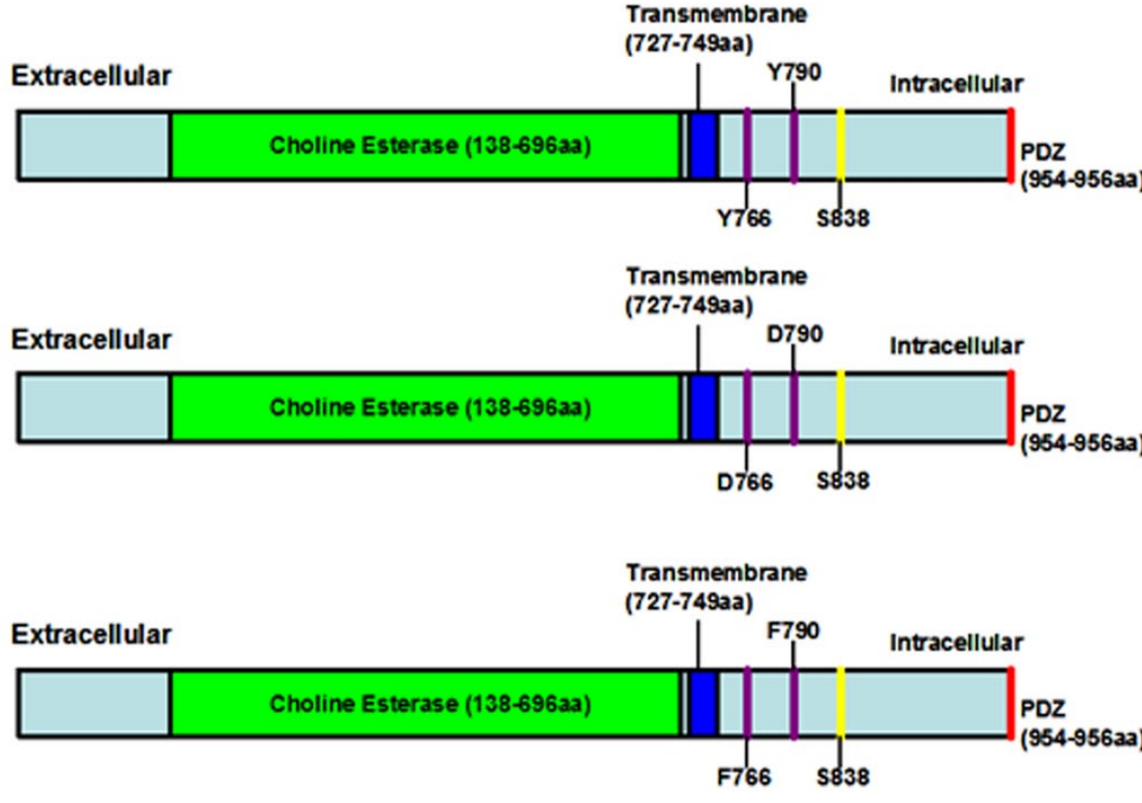

B

```
D_pseudobscura                WRNAKRQSDRFYDEDVFINGEGLEPEPDPRGVDNAHMVTNHHAMR-SRDNIYEYRDSPSSKTLASKAHT
D_grimshawi                   WRNAKRQSDRFYDEDVFINGEGMEPEPDPRGVDNAHMVTNHHAMR-SRDNIYEYRDSPSTKTLASKVHT
D_virilis                     WRNAKRQSDRFYDEDVFINGEGMEPEPDARGVDNAHMVTNHHALR-SRDNIYEYRDSPSTKTLASKAQT
D_melanogaster                WRNAKRQSDRFYDEDVFINGEGLEPEQDTRGVDNAHMVTNHHALR-SRDNIYEYRDSPSTKTLASKAHT
Culex_pipiens                 WRNAKRQSDRFYDEGVFVVDN-PESERGDVGIDNNVLQAQ--PLR---QNIYEYRDSP-SKYGKHPPPT
Aedes_aegypti                 WRNAKRQSDRFYDDGVIVVDN-PESER-DVGIDNNVLQAQ--PLR-TRDNIYEYRDSP-TKY--KSPPT
Anopheles_gambiae             WRSAKRESDRLYDEAVFGMDN-PESER-DTVMENNMLQAQ--PLRGQSGNIYEYRDSP-SKYSKMPPDG
Nasonia_vitripennis           WRNAKRQSDHYYSGDILMVRD-DEQSE---GIDN--------LTRASKENMYEYRDTPPVRARNPRNIN
Apis_mellifera                WRNAKRQSDHYYSGDILMVRD-DEPSE---GIEN--------ITRTSKENIHEYRDMPPIKSRIPR---
Bombyx_mori                   WRNAKRESDRYYADDVFVV---PEAE--DVGIDN--------INR-SRDNIYEYRDLPLKRPHT-----
Tribolium_castaneum           WRNAKRQSDRFYD---------PDPD--E-GVDN---------TRL-TS-AYDY----AEKLRTPISVP
Acyrthosiphon_pisum           WCNAKKTKDRFYNGDVLVVREEPMPMSHQ-GIDN----------RSVTSNIYEYHDAPIKTLHASPKKT
Pediculus_humanus_corporis    WRKAKRTADQFYDINLIHKED-EEGME---GVDN--------ETSQSINNIYEFREVSGSNKRPPAGTP
C_elegans                     WGN-KEDEEAAYGAENHQLVEYRDTGHSVSDATISSRTRSPRSRITNL
C_briggsae                    FGH-KEEEDAVYGESHQLVDFGIR--SVSDGTVSSRTRSPHSRI
```

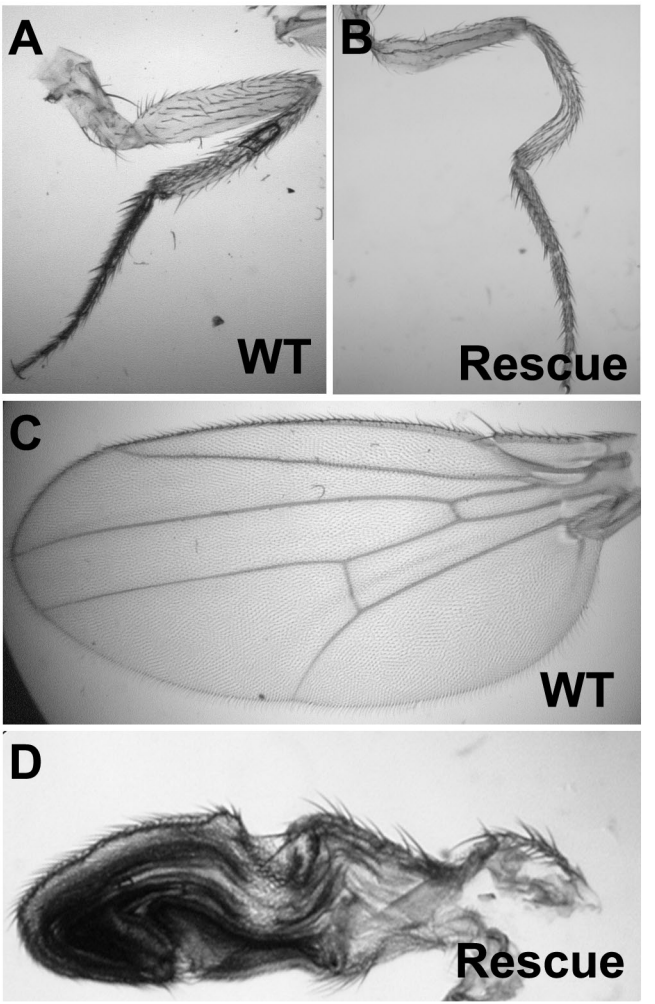
A
WT
B
Rescue
C
WT
D
Rescue

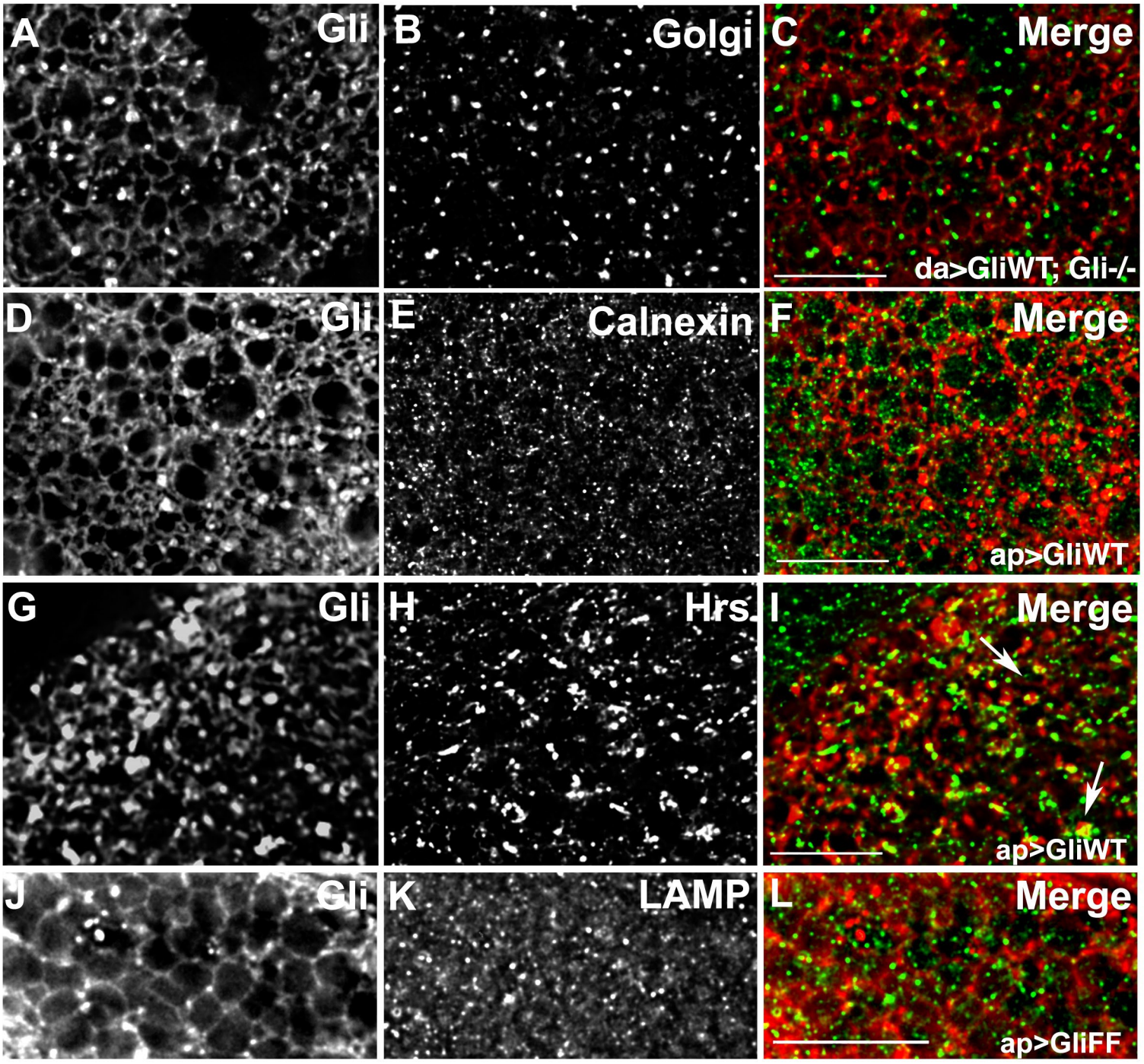
A
Gli
B
Golgi
C
Merge
da>GliWT; Gli-/-
D
Gli
E
Calnexin
F
Merge
ap>GliWT
G
Gli
H
Hrs
I
Merge
ap>GliWT
J
Gli
K
LAMP
L
Merge
ap>GliFF

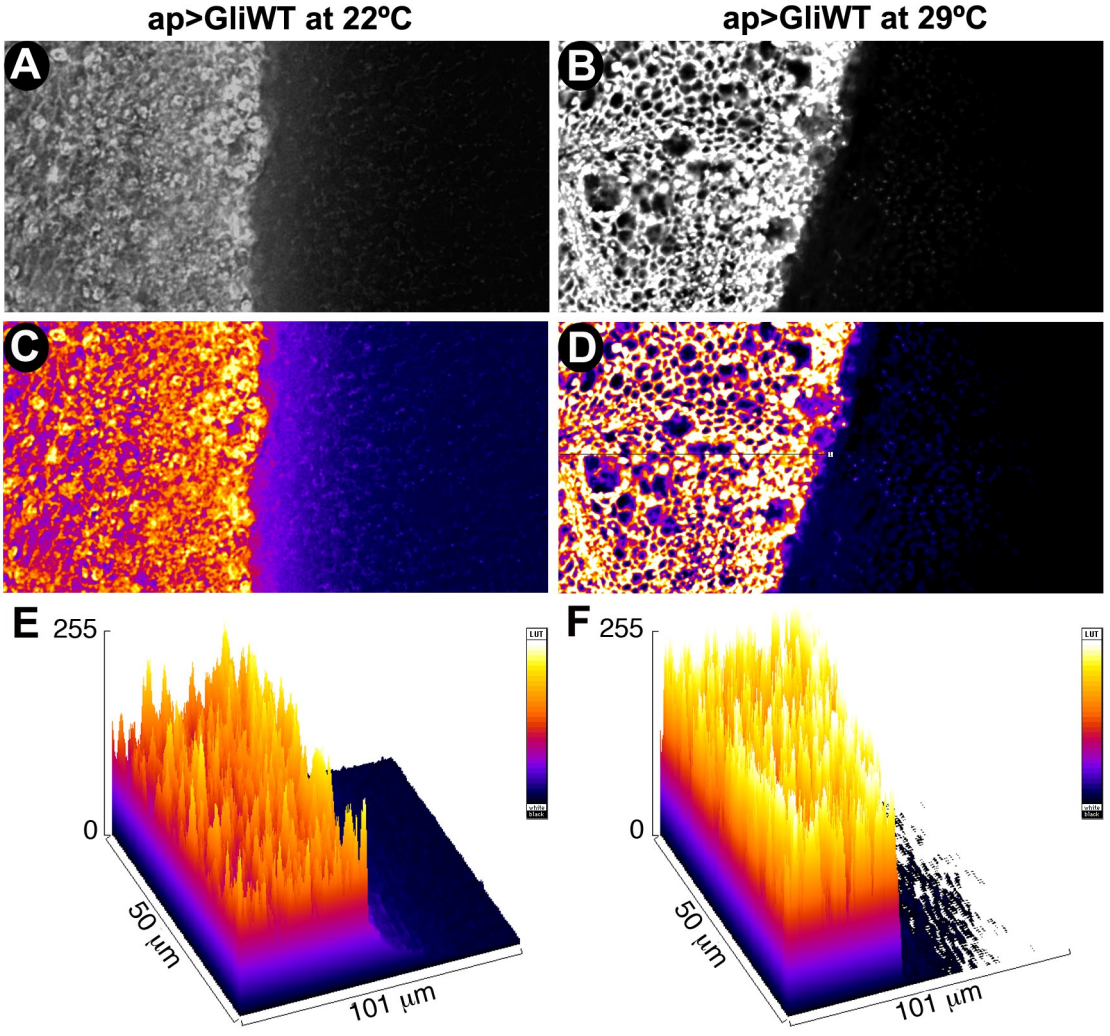
ap>GliWT at 22ºC
ap>GliWT at 29ºC
A
B
C
D
E
255
0
50 µm
101 µm
LUT
F
255
0
50 µm
101 µm
LUT

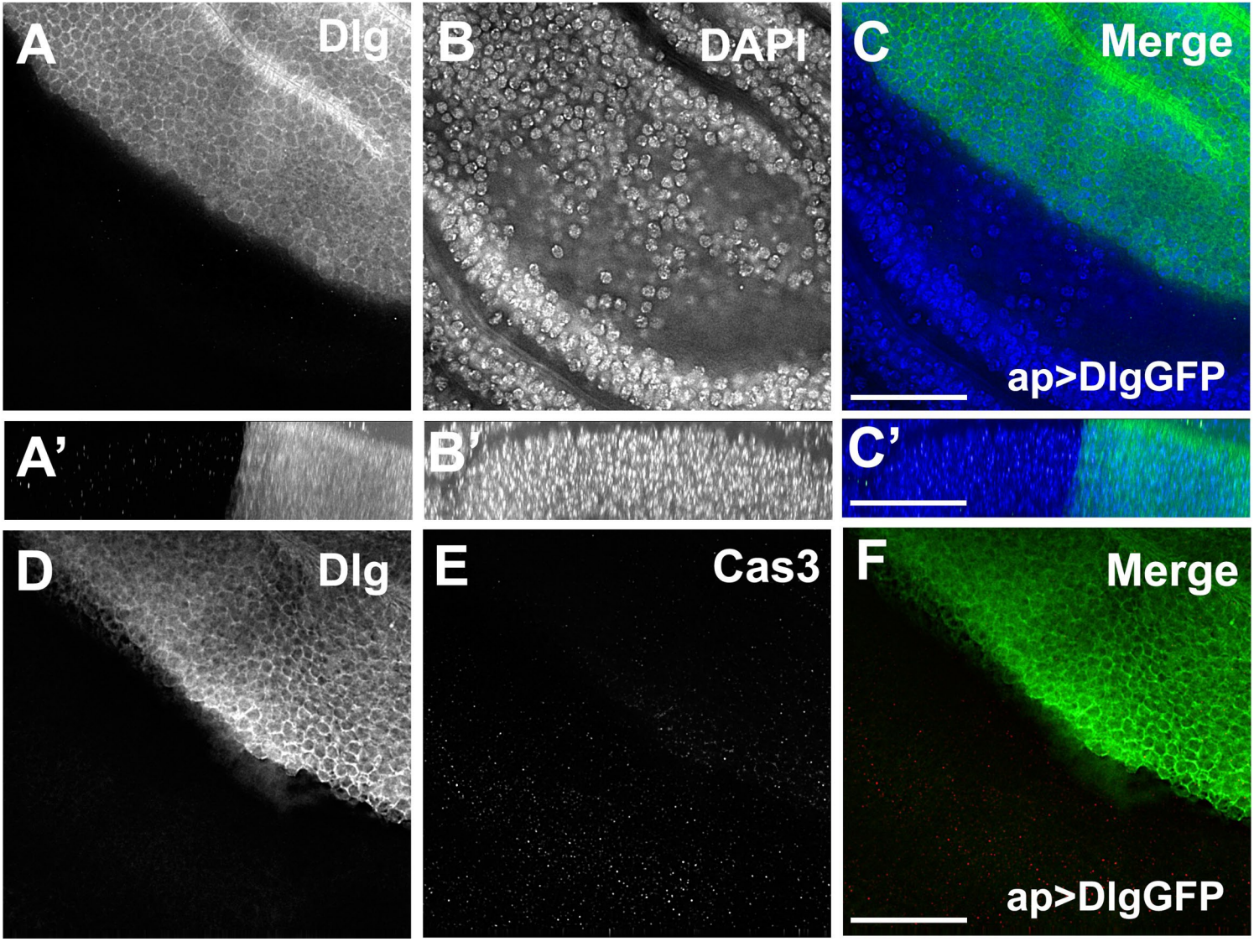
A
Dlg
B
DAPI
C
Merge
ap>DlgGFP
A'
B'
C'
D
Dlg
E
Cas3
F
Merge
ap>DlgGFP

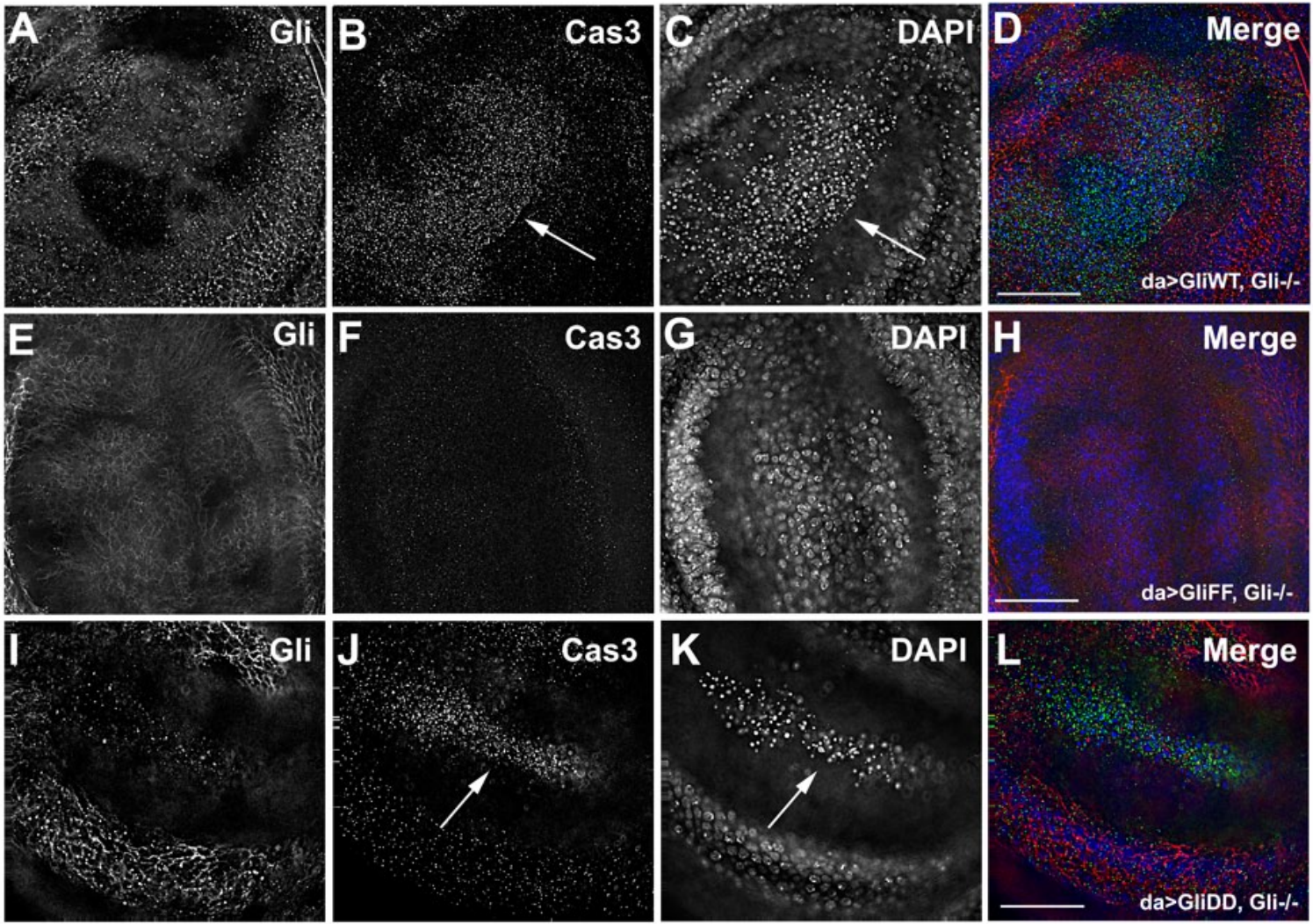
A
Gli
B
Cas3
C
DAPI
D
Merge
da>GliWT, Gli-/-
E
Gli
F
Cas3
G
DAPI
H
Merge
da>GliFF, Gli-/-
I
Gli
J
Cas3
K
DAPI
L
Merge
da>GliDD, Gli-/-